SUITABILITY OF SATELLITE RAINFALL FOR HYDROLOGICAL MODELLING IN KIKULETWA CATCHMENT, TANZANIA.

PASKALIA BAZIL LYIMO

June, 2015

SUPERVISORS:
Ir. G.N. Parodi (Gabriel)
Dr. Ir. C. Van der Tol (Christiaan)

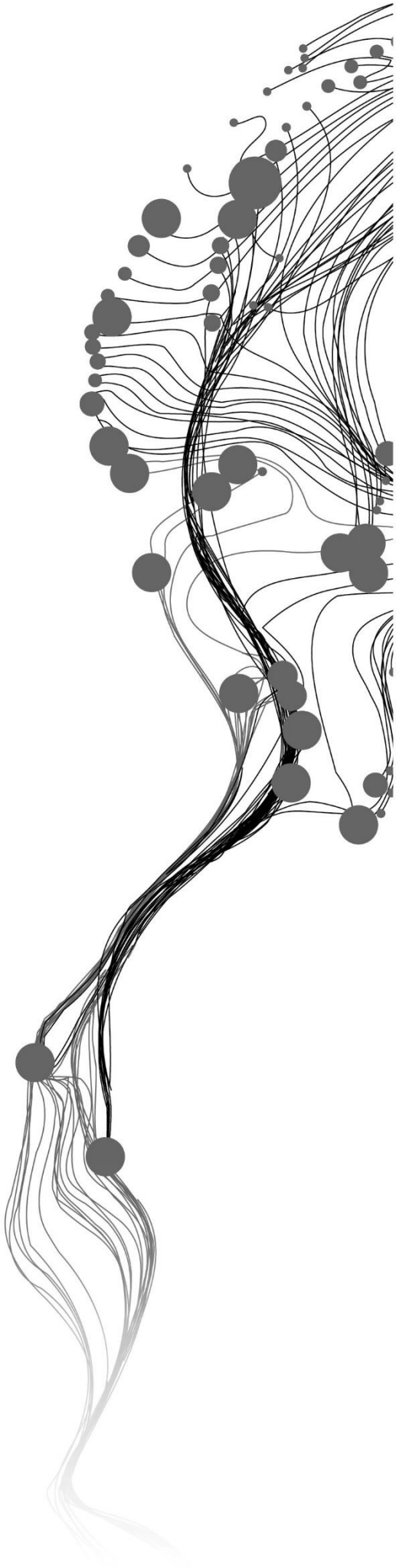

SUITABILITY OF SATELLITE RAINFALL FOR HYDROLOGICAL MODELLING IN KIKULETWA CATCHMENT, TANZANIA.

PASKALIA BAZIL LYIMO
Enschede, The Netherlands, June, 2015

Thesis submitted to the Faculty of Geo-Information Science and Earth Observation of the University of Twente in partial fulfilment of the requirements for the degree of Master of Science in Geo-information Science and Earth Observation.
Specialization: Water Resources and Environmental Management

SUPERVISORS:
Ir. G.N. Parodi (Gabriel)
Dr. Ir. C. Van der Tol (Christiaan)

THESIS ASSESSMENT BOARD:
Dr. Ir. C.M.M. Mannaerts (Chair)
Dr. D. Alkema (External Examiner, ITC – University of Twente)

Dedicated to my husband and my children

ABSTRACT

Integrated Water Resources Management especially at the catchment scale requires a timely and accurate hydro-meteorological data. These data are sometimes insufficient due to the sparse distribution of gauges or unavailability of gauges in inaccessible areas. Satellite data are potential alternative data sources in terms of spatial and temporal resolution. The aim of this study is to evaluate the suitability of satellite rainfall products from (2010 – 2014) in driving a hydrological model in Kikuletwa catchment, Tanzania. Rainfall products from TRMM/MSG-MPE and CHIRPS were compared to ground rainfall to see their ability in rainfall detection. Both products showed bias, but TRMM was selected for further processing as it has a temporal scale similar to that of ground rainfall. The Cumulative Distribution Function (CDF)-matching method was used to correct TRMM rainfall distribution within the study area. Moreover, available ground data, TRMM rainfall and potential evapotranspiration from MOD 16 were used to force the HBV-Light model.

Comparison results on a daily scale indicated the inability of all products to capture rainfall in the study area. However, monthly comparison has resulted in a good correlation coefficient of above 0.5 for the TRMM and between 0.3 and 0.5 for CHIRPS and MSG-MPE. TRMM showed the strength of capturing temporal variation of rainfall and has more hit counts as compared to other products. MSG-MPE has many missing values > 80% while CHIRPS has no missing values, but many zeros (no rain) >90%. However, MSG-MPE has overall good Probability of Detection (POD) values ranging from 0.4 - 0.7 for most of stations and sub-catchments. TRMM has good POD in three stations (0.9, 0.7 and 0.5) while other stations and sub-catchments have <0.4 POD values. CHIRPS has POD values ranging from 0.1-0.2.

Modelling results with ground and merged rainfall data showed a reasonable performance with NS of (0.8 and 0.6) and RVE of (1.4% and 2%) respectively. Uncorrected and corrected TRMM data did not perform well during model calibration with NS of 0.3 and 0.5. However, model validation results have NS values ranging from 0.01 to 0.2 and RVE of 5%, 9%, 13% and 10% for ground, merged, corrected and uncorrected TRMM rainfall.

The water balance component assessment showed that the system stores much water, which is released afterwards by the base-flow and evapotranspiration. Also different rainfall data sources resulted in different water balance components. Higher actual ET was calculated from ground rainfall data and the value has decreased in other data sets. However, little discharge has been generated from rainfall in ground observations and more discharge from other data sets.

Key words: HBV-Light model; Satellite rainfall products; Kikuletwa catchment; CDF-matching technique; Hydrological modelling; Merged rainfall data

ACKNOWLEDGEMENTS

I am so much grateful to our Almighty God for his grace which was sufficient throughout my studies and my stay in The Netherlands. Despite the medical difficulties, He has taken me through.

I would also like to give special thanks to The Netherlands Fellowship Programme (NFP) for their financial support which facilitated my studies at ITC. Furthermore, I would like to extend my appreciation to my organization, The Ministry of Water, for allowing me to participate in the study program.

I am thankful to my first supervisor, Ir. Gabriel Parodi for his encouragement, support and guidance during the entire period of the thesis work. Also, the contributions from my second supervisor Dr. Ir. Christiaan Van der Tol is highly appreciated. They have all impacted me with their modelling and research skills.

I would also like to thank the Pangani Basin Water Office for providing me with data. A special thanks goes to Mr. Riwa and Mr. Elia Bachuta for organizing my field work trip to Kikuletwa catchment and provision of all the necessary materials and information.

I am grateful to all Department members for their valuable knowledge and skills which have been shared during the entire study period. They have really opened a new opportunity in my career and I am proud to be part of ITC for 21 months. I am greatly indebted for their support which helped me toward successful completion of my study. The list will be incomplete without mentioning the student affairs staff for their assistance, support and encouragement during my difficulties. A special thanks goes to Ms. Thereza Burke for the great care and endless assistance during my visit to the hospital and assisted me with the Dutch-English translations. She was always there for me when I needed her, she is just wonderful. Moreover, I would like to thanks all WREM students and my colleagues, Ms. Jane Ndungu, Mr. Omar Bakar, Mr. Damas Mbaga and Mr. Hezron Timothy for their wise advice and support during the whole period of my study.

Lastly, but not the least in any way, I would like also to thank my family for their prayers, support and encouragement in which I believe they keep me moving. My husband especially was greatly appreciated during this time, as he came twice all the way from Tanzania for the surgeries, it really helped in the speedy recovery and was able to resume studies within a few weeks. Julian, may you be blessed abundantly and all your heart's desire be granted. Amen

TABLE OF CONTENTS

LIST OF FIGURES

LIST OF TABLES

LIST OF ABBREVIATIONS

CREST	Couple Routing and Excess Storage
CDF	Cumulative Distribution Function
CHIRPS	Climate Hazards Group Infra-Red Precipitation with Stations
DEM	Digital Elevation Model
DMSP	Defence Meteorological Satellite Program
ETa	Actual evapotranspiration
EUMETSAT	European Organization for the Exploitation of Meteorological Satellite
FAR	False Alarm Ratio
FBI	Frequency Bias Index
GDAS	Global Data Assimilation System
IUCN	International Union for Conservation of Nature
ISOD	In-situ and Online Data Toolbox
ILWIS	Integrated Land and Water Information System
HBV	Hydrologiska Byrans Vattenbalans-avdelning
KIA	Kilimanjaro International Airport
LC	Land Cover
MD	Mean Difference
MOD 16	MODIS Global Evapotranspiration Project
MW	Megawatt
MSG-MPE	Meteosat Second Generation- Multi-Sensor Precipitation Estimates
NOAA-CPC	National Oceanic and Atmospheric Administration Climate Prediction Centre
NyM	Nyumba ya Mungu
POD	Probability of Detection
PET	Potential Evapotranspiration
PR	Precipitation Radar
RS	Remote Sensing
SEVIRI	Spinning Enhanced Visible and Infrared Imager
SRE	Satellite Rainfall Estimates
SRTM	Shuttle Radar Topography Mission
SWAT	Soil and Water Assessment Tool
TMI	TRMM Microwave Imager
TMPA	TRMM Multi-satellite Precipitation Analysis
T.P.C	Tanganyika Planting Company
TRMM	Tropical Rainfall Measuring Mission
WB	Water Balance

1. INTRODUCTION

1.1. Background

In order to promote sustainable development and conservation of environmental flows, estimation of catchment water balance is needed to give an overview of periodic water availability for the purpose of water resources planning and management. Hydrological models are the useful tools which help us in understanding catchment behaviour. But their applicability is hindered by shortage of data, especially in developing countries (Mashingia, Mtalo, & Bruen, 2014).

Rainfall is the main input into hydrological models and as such its accuracy of measurement from network of stations determines to a considerable extent reliability of water balance computation. Rainfall is a hydro-meteorological variable and it is difficult to measure due to its greater temporal and spatial variability (Jeniffer, Su, Woldai, & Maathuis, 2010). However, ground measuring networks (rain gauges) in catchments are either sparsely distributed or do not exist at all (Behrangi, Lebsock, Wong, & Lambrigtsen, 2012).

Satellite based precipitation products have advantages over ground based observations in terms of spatial and temporal resolution. They act as a potential alternative data sources for data sparse or un-gauged basins. Also, the recent technical development has largely improved their applicability as rainfall alternative input to ground based rainfall in large scale distributed hydrological models (Stisen & Sandholt, 2010).

Water resources management challenges in basins of Sub-Saharan Africa, particularly Tanzania, are increasing due to rapid urbanization, poverty and food insecurity. This also applies in Kikuletwa sub-catchment located in the north-western part of the Pangani River Basin in Tanzania. It is drained by 15 major rivers originating from Mount Kilimanjaro and Mount Meru. These rivers join to form the main Kikuletwa River before entering the Nyumba ya Mungu (NyM) reservoir. The river is the main source of water to Nyumba ya Mungu regulated reservoir having a power plant producing 8 MW (Mwamila, Kimwaga, & Mtalo, 2008).

The water users within the catchment include small scale subsistence farmers, two cities (Arusha and Moshi), small towns, commercial farms, pasture and mines. Rapid population growth causes demand for land to increase within the area. People living along the slopes of the mountains are now intensively farming their land by utilizing most of the water originated from the highlands. As a result, the volume of water flowing in the river has decreased. The decrease in the volume of water has been the source of competition and conflicts among water users. This also causes wetlands and perennial rivers to dry up (IUCN, 2009).

To overcome the challenges of water resources management in the country, the Ministry of Water through the support of the Development Partners is funding an Integrated Water Resources Management and Development plans (IWRMD) in all nine river basins including Kikuletwa sub-catchment. Another initiative towards sustainable management of water resource which is done by the Ministry through river and lake basins is the water allocation system. Pangani Basin Water Board (PBWB) is responsible for registering and issuing of water use permits within the basin. On the other hand, water allocation activities also requires the assessment of the available water in order to ensure its sustainability. Thus, all these studies require hydro-meteorological data which are sometimes not available. Therefore, this study will give an insight on the suitability and reliability of satellite rainfall for hydrological and other catchment studies.

1.2. Problem Statement

Kikuletwa sub- catchment is in the upper part of the Pangani River Basin forming the head water of the Pangani River flowing to the NyM reservoir. There is an extensive network of river gauging and meteorological stations within the sub-catchment, however many of these stations have not operated for a long time. In some cases, stations have stopped running just after two years of operation and little has been done to return them into service. In addition, most of the stations are located in the northern part of the sub-catchments which causes difficulty in estimating rainfall in the southern part. All those problems compromise the collection and management of data which leads to scarcity of data within the area. The absence of adequate hydro-meteorological data have been the cause of obvious concern amongst the professionals in the Pangani River Basin (IUCN, 2009). This is because hydrological and environmental studies require adequate and reliable data for their successful completion.

Water resources planning and management especially at catchment scale requires timely and accurate hydro-meteorological data. These data are normally used to study and understand catchment behaviour through hydrological models. However, development of such comprehensive models require substantial amount of resources, i.e. observation data like rainfall (Ndomba, Mtalo, & Killingtveit, 2008). A few studies have been conducted in the catchment which mainly focus on the comparison of satellite and ground rainfall data, others being climate change and evaluation of catchment services studies. Comparatively, little has been done to find an alternative data sources for the aforementioned studies. Therefore, this study will address the fitness of satellite based rainfall information as an alternative data sources to be used in hydrological modelling.

1.3. Thesis Objectives

1.3.1. Main Objective

The main objective of this research is to evaluate if satellite rainfall data could be used to improve the quantification (assessment) of stream flow in the Kikuletwa sub-catchment.

1.3.2. Specific Objectives

i. To assess the relation between ground and satellite rainfall estimates: spatial distribution adequacy and matching.

ii. To evaluate inadequacies between the hydrograph data and the rainfall (ground, TRMM/MSG-MPE and CHIRPS).

iii. To evaluate the simulated hydrograph in terms of water balance, shape and main characteristics as calculated from the HBV model in relation with input rainfall data in order to see the adequacy of TRMM/MSG-MPE and CHIRPS in modelling.

1.3.3. Research Questions

i. How does satellite rainfall data correlates with measured ground rainfall data?

ii. Does the agreement between rainfall and discharge measured sufficient to allow hydrologic modelling?

iii. Is there any difference in water balance components when using satellite and ground rainfall data?

1.4. Significance of the Study

This study has a large societal and economic importance as the Kikuletwa River drains the upper part of the catchment to NyM reservoir which is used for hydroelectric power generation (8 MW). There is also

agriculture, household, mining and small scale industries which depends on the water from this river. The results of this study will show the suitability of Satellite data in the eventual calibration of hydrological model, which, in turn, will improve planning and management of water resources. If successful, the results obtained will aid in decision making as the overall water balance of the sub-catchment can be obtained.

1.5. Thesis Outline

This thesis has six Chapters. A brief background of the study, statement of the problem, research objectives, research questions and significance of the study have been addressed in chapter one.

Chapter two deals with literature review, it explains what other researchers have done in the field of hydrological modelling by using satellite rainfall products and other related studies.

Chapter three describes the study area and explains about materials which have been used.

Chapter four gives detailed methodologies used.

Chapter five gives details of the results obtained followed by discussion of those results.

Chapter six concludes the study and gives further recommendations.

2. LITERATURE REVIEW

2.1. Remote Sensing Rainfall Estimation

Rainfall is an important component in the hydrologic cycle varying greatly in time and space. Knowledge of its amount is essential to the society in various fields like weather forecasting and hydrological studies. Measurements of rainfall by using conventional instruments (gauge) has some difficulties, especially in places where there is uneven distribution of rain gauges or places where there are no gauges (Kidd & Levizzani, 2010).

Satellite based precipitation estimates with high temporal and relatively high spatial resolution provides a potential alternative source of forcing data for hydrological models in regions where conventional ground precipitation measurements are sparsely located or unavailable (Su, Hong, & Lettenmaier, 2008).

Various techniques have been developed to estimates rainfall from different sensors. The retrieval methodologies fall into three categories based upon type of observation, primarily Visible/Infrared (VIS/IR), Microwave (MW) channels and Multi- sensor or Blending techniques (Kidd & Levizzani, 2010). The techniques are explained below.

2.1.1. Visible/Infrared Techniques (VIS/IR)

VIS/IR sensors mounted on geostationary satellite like MSG and GOES were the first to be conceived. They are simple to apply while at the same time they have been proven with relatively low accuracy. Rainfall can be retrieved from VIS images since bright clouds tend to be thick, and thick clouds are more likely to be associated with rainfall. However there is a weak relationship between brightness and rainfall, which necessitate the use of other observation (TIR) in conjunction with VIS. TIR imagery that measures the thermal emission from cloud top particles is more frequent as it works day and night. It based on the assumption that, heavy rainfall is associated with large, taller clouds with colder cloud tops. It is suggested that by observing the cloud top temperature a simple rain estimate can be derived. This method is indirect with significant variations in the relationship during the lifetime of a rainfall event, between rain systems and between climatological events (Kidd & Levizzani, 2010).

2.1.2. Microwave Techniques (MW)

Microwave sensors on board low earth orbiting satellites, such as TRMM Microwave Imager (TMI) provide acceptable estimate of rainfall. This is because at MW frequencies, precipitation particles are the main source of attenuation of the upwelling radiation. Therefore, MW techniques are physically more direct rainfall estimation as compared to VIS/IR techniques. The main limitation of this method is due to its low temporal and spatial resolution of the data (Kidd & Levizzani, 2010).

2.1.3. Multi-sensor or Blending Technique

A number of techniques have been developed to exploit the synergy between the polar orbiting (MW rainfall retrievals) and geostationary (IR retrievals). The main purpose of merging these data is to try to take advantage of strengths of both techniques. Those techniques include TRMM Multi-satellite Precipitation Product (Huffman et al., 2007a) and Climate Prediction Centre (CPC) morphing method (Joyce, Janowiak, Arkin, & Xie, 2004). Different studies have been conducted by using this technique and came to conclusion that combining IR and MW improves rainfall estimation. A good example is the study by Mutiga, (2011) who estimated spatial temporal rainfall distribution in Makanya catchment, Tanzania by

using blended approach. She uses IR channel from Geostationary MSG with the low earth orbiting passive TRMM Microwave Imager (TMI). The results were compared with the available ground data and gave a good correlation of about 80%.

Another study on the comparison of rainfall from the TRMM 3B42, Multi-Sensor Precipitation Estimate-Geostationary (MPEG) and the Climate Forecast System Reanalysis (CFSR) with ground observed data was performed in the Lake Tana basin, Ethiopia by Worqlul et al., (2014). They tested the accuracy of both products with the available 38 ground stations in 2010 and the results showed that the MPEG and CFSR provided the most accurate rainfall estimates of 78 and 86 % respectively of the observed rainfall while TRMM explained only 17% of the variation.

2.2. Hydrological Remote Sensing in Kikuletwa Sub-catchment

There is little literature on the use of Satellite based products on hydrological modelling in the Kikuletwa sub catchment. The available related literature focuses on the comparison of satellite based rainfall and gauge rainfall (Mashingia et al., 2014) (Haque, Maskey, Uhlenbrook, & Mul, 2013). Other studies looked at Climate Change and decline in water resources in Kikuletwa sub catchment (Linus & Pudensiana, 2014), Catchment Ecosystems and Downstream water (IUCN, 2009), evaluating watershed services availability under future management and Climate Change scenarios (Notter, Hurni, Wiesmann, & Ngana, 2013).

Mashingia et al., (2014) did a study on the validation of remotely sensing rainfall over major climatic regions in Northern Tanzania. They compared Tropical Rainfall Measuring Mission (TRMM) and National Oceanographic and Atmospheric Administration Climate Prediction Centre (NOAA-CPC) African rainfall estimation RFE2 with gauge rainfall. Both products exhibit relatively good correlation coefficient values of 0.81 for TRMM and 0.76 for RFE2. The results of the comparison indicate that the Satellite Rainfall Estimates (SRE) products performed reasonably well in detecting the occurrence of rainfall. Furthermore, Haque et al., (2013) conducted a study on validation of TRMM rainfall in Pangani River Basin in Tanzania. The correlation coefficient between gauge and satellite rainfall ranged between 0.67– 0.77 within sub-catchments. This indicates that satellite data can play an important role in data sparse region as well as places where gauge measurements are not available due to inaccessibility.

The main focus of the previous studies was the comparison of satellite and gauge rainfall data. However, the reliability of satellite based rainfall in hydrological modelling is still unknown. Therefore, this study is intending to fill the observed gap and develop a tool (model) which will help in fully understanding the catchment behaviour and assist in informed decision.

The previous studies on RS and ground rainfall relationship build the basis for this study as they help to discover statistical knowledge and methodologies which might be appropriate and useful during the study. Similarly, Mashingia et al., (2014) recommended in the research about validation of high resolution satellite rainfall and their applicability in hydrological modelling. Therefore, results obtained from this study will address some of the concerns raised by previous researchers.

2.3. Water Resources Modelling

Water resource modelling is an important tool for water resources planning and management especially in sparsely gauged catchments. Models contributes to a better understanding of hydrologic parameters and variables and their interactions at a catchment scale. Different modelling approaches exist which are used in water resources and environmental studies. The major categories are lumped and distributed hydrological models. They are differentiated in the way the catchment is discretized and the requirement of input data. However, spatially distributed inputs are required by these models in order to reflect the heterogeneity of the catchments (Meng, Li, Hao, Wang, & Shao, 2014a). Satellite meteorological observations have played an important role in water resources modelling especially in poorly gauged

catchments. For example Su et al., (2008) conducted a study on the hydrological prediction in poorly gauged La Plata Basin by using monthly TRMM rainfall data and concluded that the simulated results were able to capture the flooding events and to represent low flows. Another study is by T. H. M. Rientjes et al., (2011) who used HBV-96 model and land cover data from satellite to assess the effects of land cover on stream flow in the Blue Nile basin, Ethiopia. They concluded that there is a significant change of stream flow due to land cover change in that region. All these results show that hydrological modelling can help us understand the catchment's behaviour and it's response to changes of natural or anthropogenic activities which can threaten the availability and sustainability of water resources.

2.4. HBV-Light Model

HBV-Light model is a conceptual, semi-distributed hydrological model that simulates the daily discharge using daily precipitation, air temperature and estimates of monthly long-term potential evapotranspiration rates (J. Seibert & Vis, 2012). The model uses sub-basins as the primary hydrological units. It also takes into account a limited number of area-elevation distribution and little, but relevant basic land use categories.

The large number of applications using this model, under various physiographic and climatological conditions has shown that its structure is very robust and general in spite of its relative simplicity. A good example is the study on the calibration of a semi-distributed hydrological model (HBV-Light) using discharge and remote sensing data by Muthuwatta et al., (2009). The study was conducted in the Karkher River basin in Iran and the results showed that the overall discharge behaviour was well simulated. Another study is by Nebiyu Solomoni, (2013) in the Birr Watershed in Ethiopia. He uses HBV-Light model in stream flow simulation based on both ground and satellite based products. The results revealed that the model was able to simulate well the stream flow with NS and r^2 of 0.7 and 0.59 respectively.

2.5. Similar Work

A number of studies have been conducted to assess the capability of satellite based rainfall in hydrological modelling. For example, Meng, Li, Hao, Wang, & Shao, (2014) did a study on the suitability of Tropical Rainfall Measuring Mission (TRMM) rainfall in driving a distributed hydrological model in Yellow River by using the CREST model. Findings indicate that the TRMM Multi-satellite Precipitation Analysis (TMPA) rainfall performs quite well. Another study was conducted in Congo River Basin by Beighley et al., (2011). They were assessing the applicability of three satellite derived precipitation datasets (TRMM, CMORPH and PERSIANN) in driving Hillslope River Routing model. TRMM provides the best agreement to the historical stream flow data while CMORPH and PERSIANN resulted in large annual stream flow error.

3. STUDY AREA AND MATERIALS

3.1. Study Area

3.1.1. Geographic Location

Kikuletwa sub- catchment lies between latitude 3˚.03′ S – 4˚.07′ S and longitude 36˚.33′ E – 37˚.42′ E with an approximate area of **7280 km².** It is among of the five sub-catchments of the Pangani River Basin located in the Northern part of Tanzania (Figure 3.1). It covers parts of six administrative districts in Arusha, Manyara and Kilimanjaro regions (Ndomba et al., 2008).

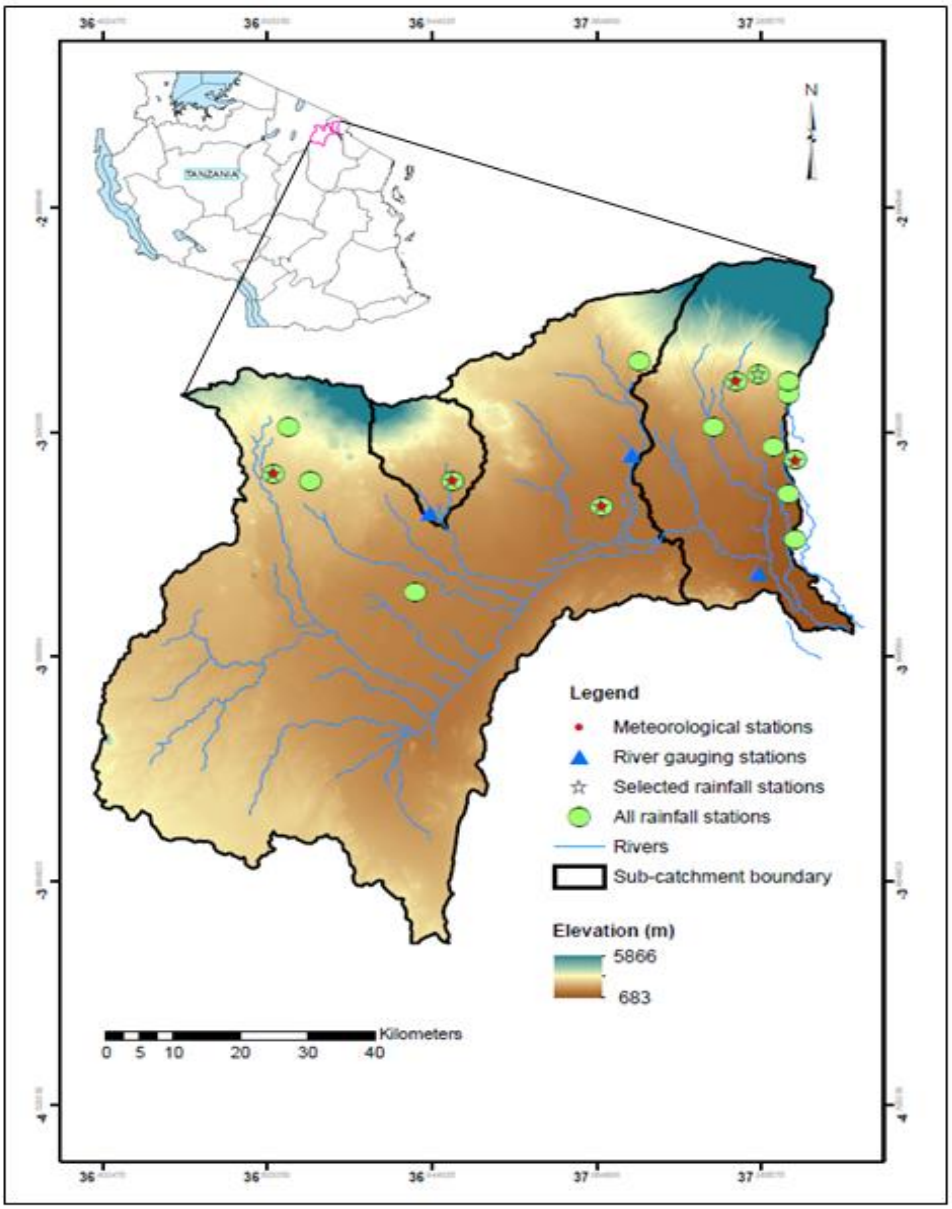

Figure 3.1: Location of the Study area and the distribution of hydro-meteorological stations

3.1.2. Topography

The altitude ranges between 683 and 5825 m above the mean sea level (m-asl). The Mountain slopes of Mt. Kilimanjaro are categorised into five ecological zones. The lower slopes (900-1800 m-asl)), the forest (1800-2800 m), the health and moorland, the high land desert (4000-5000 m-asl), and the summit (above 5000 m-asl). The low land plain lies below an altitude of 900 m classified as tropical savannah including the Maasai Steppes (Ndomba et al., 2008).

3.1.3. Climatic Characteristics

The climate of the catchment is affected by the seasonal migration of Intel Tropical Convergence Zone (ITCZ). The ITCZ of the Northeast Trade Winds and Southeast Trade Winds forces uplift of moist air, resulting in a band of heavy precipitation around the Equator, which causes is typically the bimodal rainfall pattern with two distinct rainy seasons, the short rains (October-December) separated from the long rains (March-May). The period June-September is generally the dry season with the August being the driest month (Ndomba et al., 2008).

Variation in the local climatic conditions is related to topography, as more than 50% of the sub-catchment including the lowland plain is arid or semi-arid with a mean annual rainfall of 500-600 mm $year^{-1}$. Moderate to high rainfall (1000-2000 mm $year^{-1}$) are on the southern slope of Mt. Kilimanjaro. Temperatures gradients to altitude with minimum and maximum daily temperature ranges being 12 to 17°C and 32 to 35 °C respectively (Ndomba et al., 2008). However, potential evaporation data show a gradual spatial variation as compared to other climatic data. Generally the monthly potential evaporation within the catchment is uniform except for the months of October – March where potential evaporation is very high (IUCN, 2009).

3.1.4. Land Cover and Land use

The catchment is characterised by different land cover types varying from forests on the mountain slopes, woodlands, bushlands with emergent trees, swamps to arid grassland which reflects differences in altitude and precipitation. The main cultivated crops include bananas, maize, coffee, flowers and sugar cane. Irrigated agriculture is mostly practised in the lowlands where rainfall amount is minimal. This lead to the construction of irrigation furrows as the way of getting water from a natural watercourse (IUCN, 2009).

3.1.5. Hydrology

The catchment is drained by 15 major rivers (Figure 3.1) originating from Mount Kilimanjaro and Mount Meru. They include River Kikuletwa which drains Mt. Meru through Shamabarai swamps before being joined by Rivers Weruweru, Karanga and Kikafu to form the main River Kikuletwa which flows into the Nyumba ya Mungu reservoir (IUCN, 2009). In addition, the water resources in the sub-catchment are a complex surface and groundwater system of rivers, springs and swamps. The major springs which feed the river system includes the Kware, Rundugai and Chemka contributing about 90% of the dry season river flows downstream in the Kikuletwa River (IUCN, 2009).

3.2. Materials

Two types of data sets are used in this study. Ground data collected from the Pangani Basin Water Office during field work and Satellite data, such as rainfall and evapotranspiration, which were retrieved using the In-situ and Online Data (ISOD) Toolbox in ILWIS. Digital Elevation Model (DEM) has been downloaded from the Shuttle Radar Topographic Mission (SRTM) website while Land Cover map was obtained from the Ministry of Water.

During fieldwork I interviewed some of the Pangani Basin staff and gauge readers about the background of the catchment and how do they record, store and manage hydro-meteorological data. They responded by saying that in the past, the catchment was having an extensive network of hydro-meteorological stations. That system no longer exists due to several factors such as the destruction of the stations by heavy rains, animals, erosion of the banks, siltation or vandalism. Others are instruments failure and it take too long to be fixed. All these problems affect measurements as some of the stations have been removed or covered by silt and marks are no longer visible. This brings errors while reading and a lot of gaps in the hydro-meteorological data. Moreover, Appendix B shows some of the newly installed hydro-meteorological stations visited during the field work. They are part of the Water Sector Development Program, which is currently implemented by the Ministry of Water in all rivers and lake basins in Tanzania.

3.2.1. Ground Data

i. Discharge data

Time series of daily average discharge data for 1DD1 station located at the outlet of the catchment is available from 2010-2014. Table 3.1 below gives the summary of the station.

Table 3.1: Discharge Station

Station ID	Station Name	Lat.	Long	Elevation(m)	Period
1DD1	Kikuletwa at T.P.C	-3.57	37.34	698	2010-2014

ii. Meteorological data

Daily rainfall data from 2010-2014 for the six selected rainfall stations which are located inside and near the catchment is available for this study. Their spatial distribution is representative of the catchment's elevation. The station located in 813 m providing an indication of the amount of rainfall in the low lands while those located above 1300 m provides an indication of the amount of rainfall happening in the high lands. Temperature data for the same period is also available for three stations located within the catchment. The descriptions of the meteorological station are given in Table 3.2 below.

Table 3.2: Meteorological stations

Station ID	Station Name	Lat.	Long	Elevation (m)	Period
9337004	MOSHI AIRPORT	-3.35	37.33	813	2010-2014
9337115	KIA	-3.42	37.07	891	2010-2014
9337021	LYAMUNGO	-3.23	37.25	1250	2010-2014
9337121	OSAKI	-3.22	37.28	1344	2010-2014
9336033	ARUSHA	-3.37	36.63	1387	2010-2014
9336035	TENGERU	-3.38	36.87	1136	2010-2014

3.2.2. Satellite Data

i. Rainfall from Tropical Rainfall Measuring Mission (TRMM-3B42 V7)

TRMM is designed to measure tropical precipitation and its variation from a low-inclination orbit combining a suite of sensors to overcome many of the limitations of remote sensors previously used for such measurements from space. It has the global coverage of 50^0 S to 50 ^{0}N latitudes and 180^0 W to 180^0 E longitudes. TRMM 3B42 v7 is one of the algorithm which is able to make use of data from the TRMM mission. Its purpose is to produce TRMM-adjusted merged IR precipitation and root mean square precipitation error. The TRMM 3B42 v7 obtains its input from two different types of sensors, namely passive microwave (PWM) and Thermal Infra-red (TIR). PMW data which come from the TRMM Microwave Imager (TMI), Special Sensor Microwave/Imager (SSM/I), Advance Microwave Scanning Radiometers-Earth Observing System (AMSR-E), The Advanced Microwave Sounding Unit–B (AMSU-B) and the Microwave Humidity Sounders (MHS) while IR data come from geosynchronous earth orbit (GEO) satellites.

The rainfall estimates are produced following four steps:

a) All microwave estimates are combined,

b) IR estimates are created with microwave calibration,

c) PMW and IR data are combined in which IR estimates are used to fill the gaps in PMW rain rates and

d) Re-scaling of TRMM precipitation estimates with monthly rain gauges to remove bias and create the final TRMM product.

The TRMM-3B42 v7 rainfall data are available from 1998 to date with daily temporal and approximately 27.83 km spatial resolution (Huffman et al., 2007a).

ii. Rainfall from Meteosat Second Generation - Multi Sensor Precipitation Estimates (MSG-MPE)

MSG-MPE is an algorithm which combines the passive microwave rain rates from polar orbiting satellite with TIR data from EUMETSAT geostationary satellites. It is generated over the regions up to 60° longitudes and 60° latitudes and uses data from Special Sensor Microwave/Imager (SSM/I) on board the polar orbiting Defence Meteorological Satellite Program (DMSP) to continuously re-calibrate the retrieval function of geo-stationary IR-imagery. Its primary goal was to combine the advantages obtained from both retrieval systems in order to generate comprehensive and near real time information. The idea was successful as they managed to produce instantaneous rain-rates of higher temporal resolution of 15 min in an original MSG pixel resolution of 3 km (Heinemann & Kerényi, 2003). The MSG-MPE time series data are available from 2007 to present. The images are freely available via their website and can also be retrieved in ILWIS through In-situ and Online Data Toolbox (ISOD).

iii. Rainfall from Climate Hazards Group Infra-Red Precipitation with Stations (CHIRPS)

CHIRPS rainfall data set was developed by the U.S. Geological Survey (USGS) and the Climate Hazards Group at the University of California, Santa Barbara, is a blended product combining the monthly precipitation climatology, quasi-global geostationary thermal infrared (TIR) satellite observations from two National Oceanic and Atmospheric Administration (NOAA) sources, the Climate Prediction Center (CPC) and the National Climatic Data Center (NCDC). Atmospheric model rainfall field from the NOAA Climate Forecast System version 2 (CFSv2) and ground precipitation observations from national and regional meteorological authorities. Pentadal rainfall estimates, created from satellite data based on Cold Cloud Duration (CCD) based on regression models calibrated using TRMM, are expressed as percent of normal and multiplied by the corresponding precipitation climatology. Next, stations are blended with this CHIRP data to produce CHIRPS. Quasi-global gridded products covering 50^0 N to 50^0 S Latitude and all Longitude are available from 1981 to two months before present at 5 km spatial resolution and at

pentadal, dekadal, and monthly temporal resolution. Daily values are available for Africa, which were created by using daily cold cloud duration percentage (Funk et al., 2014).

iv. MODIS Potential Evapotranspiration Data Set (MOD 16)

The MODIS Global Evapotranspiration Project (MOD 16) is a part of the National Aeronautics and Scape Administration/Earth Observing System (NASA/EOS) project to estimate global terrestrial evapotranspiration from the earth's surface by using remote sensing data. It produces global evapotranspiration, latent heat flux, potential evapotranspiration and potential evapotranspiration (PET). The data sets cover the period from 2000-2014 at 1 km spatial resolution with the 8 days, monthly and annual time interval. These data sets are estimated using Mu et al. improved ET algorithm (2011) which is based on Penman-Monteith equation (Mu, Zhao, & Running, 2011). The Penman-Monteith equation reads;

$$\lambda E = \frac{sA + \rho Cp\ x\ (e_{sat} - e)/r_a}{s + \gamma\ x\ (1 + r_s/r_a)} \quad (3.1)$$

Where λE is the latent heat flux and λ is the latent heat of evaporation; s = d (e_{sat})/dT, the slope of the curve relating saturated water vapour pressure (e_{sat}) to the temperature; A is the available energy partitioned between sensible heat, latent and ground heat fluxes on the land surface; ρ is air density, C_p is the specific heat capacity of air; and r_a is the aerodynamic resistance. The psychometric constant is given by γ = Cp x P_a x M_a / (λ x M_w), where M_a and M_w are molecular masses of dry and wet air respectively and P_a is atmospheric pressure. Table 3.3 presents the summary of the satellite data used in this study.

Table 3.3 : Summary of the satellite data used

Data	Product	Resolution		Coverage		Period
		Spatial	Temporal	Lat.	Long.	
Rainfall	TRMM-3B42 v 7	27.8 km	Daily	50° N - 50° S	180° W - 180° E	1998 - To date
	MSG - MPE	3 km	Daily	60° N - 60° S	60° W - 60° E	2007 - To date
	CHIRPS	5km	Daily	Africa		1981- To date
PET	MOD 16	1 km	8 days	Global		2000 -2014
DEM	SRTM	90 m				2000

3.2.3. HBV-Light Model

HBV-Light Model has been selected for this study. It is a conceptual model that applies a semi-distributed model domain. Water storage and fluxes inside the model are tracked and thus the water balance is conserved (J. Seibert & Vis, 2012).

The HBV-Light model is a semi-distributed hydrological model, which means that a catchment can be separated into different elevation and vegetation zones as well as into different sub-catchments. Upstream sub-catchments are linked to downstream sub-catchments and thus runoff behaviour from the interconnected sub-catchments can be simulated.

The model consists of four routines namely snow routine, soil moisture routine, response routine and routing routine as shown in Figure 3.2 below. Since there is no snow in the study area, snow routine has been ignored in this study. It can be seen from the diagram that shallow soil layers in the catchment are represented by a series of boxes (i.e. soil water stores). There are also two storages that represent the

deeper part of the real world. This deeper part consists of shallow subsurface and deeper subsurface that remains saturated (i.e. ground water).

Precipitation causes infiltration and water storage in the shallow unsaturated soil store. Increased storage causes generation of downward flow process that recharge the shallow subsurface store. From this zone percolation occurs that recharge the deeper saturated subsurface. The stream flow in a channel is the result of a number of interacting flow processes that make up hydrological cycle. As the flow of water in HBV model is from the land surface to the lower zone store, for each store a water balance applies that keeps track of the storage volume, the incoming and outgoing fluxes (J. Seibert & Vis, 2012). Generally, the water balance that is solved in the approach can be described as:

$$P - E - Q = \frac{d}{dt}(SP + SM + UZ + LZ + LAKES) \quad (3.2)$$

Where,

P = Precipitation

E = Evapotranspiration

Q = Runoff

SP = Snow pack

SM = Soil moisture

UZ = Upper ground zone

LZ = Lower ground zone

Lakes = Lake Volume

Kikuletwa catchment is divided into three interconnected sub-catchments. The discretisation was done during The Pangani River Flow Assessment study, which was conducted by the International Union for Conservation of Nature (IUCN) and the Pangani Basin Water Office, based on similarity in terms of hydrology, geomorphology and chemistry (IUCN, 2009). Inflow from the connected sub-catchments will be added to the local runoff computed by the model to yield total stream flow. Each sub-catchment has different land covers and elevation in which all will be represented in the model. It is characterised by volcanic soil with high organic contents and amorphous clay which increase its water holding capacity. Moreover, the catchment has a surface and groundwater interactions, which is seen in the observed discharge data. Base flow comprises a large part of the total runoff and even flows during dry season. Based on the catchment description above and manifest fit and readiness of the model, HBV-Light model was chosen to simulate runoff in that catchment.

HBV-Light model has different model structures like, the standard version, three groundwater boxes, different response function (delay) and one groundwater box in which catchment characteristics determine the structure to be used. More information about this model can be found in Jan Seibert, (2005).

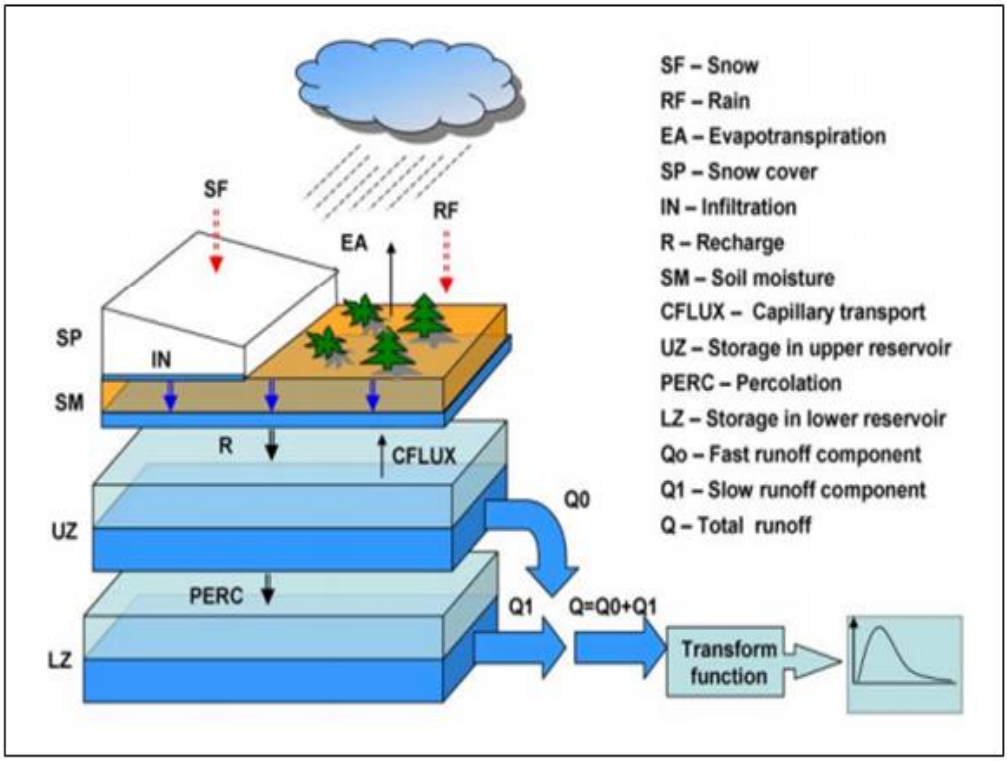

Figure 3.2: Schematic Structure of HBV-Light model (Solomatine & Shrestha, 2009)

4. RESEARCH METHOD

Figure 4.1 presents different methods which have been employed in the first part of the work to achieve the stated objectives of this study. Steps followed during hydrological modelling are presented in the next section. Both ground and satellite rainfall data have been subjected to a consistency data quality check and analysis before been used in modelling.

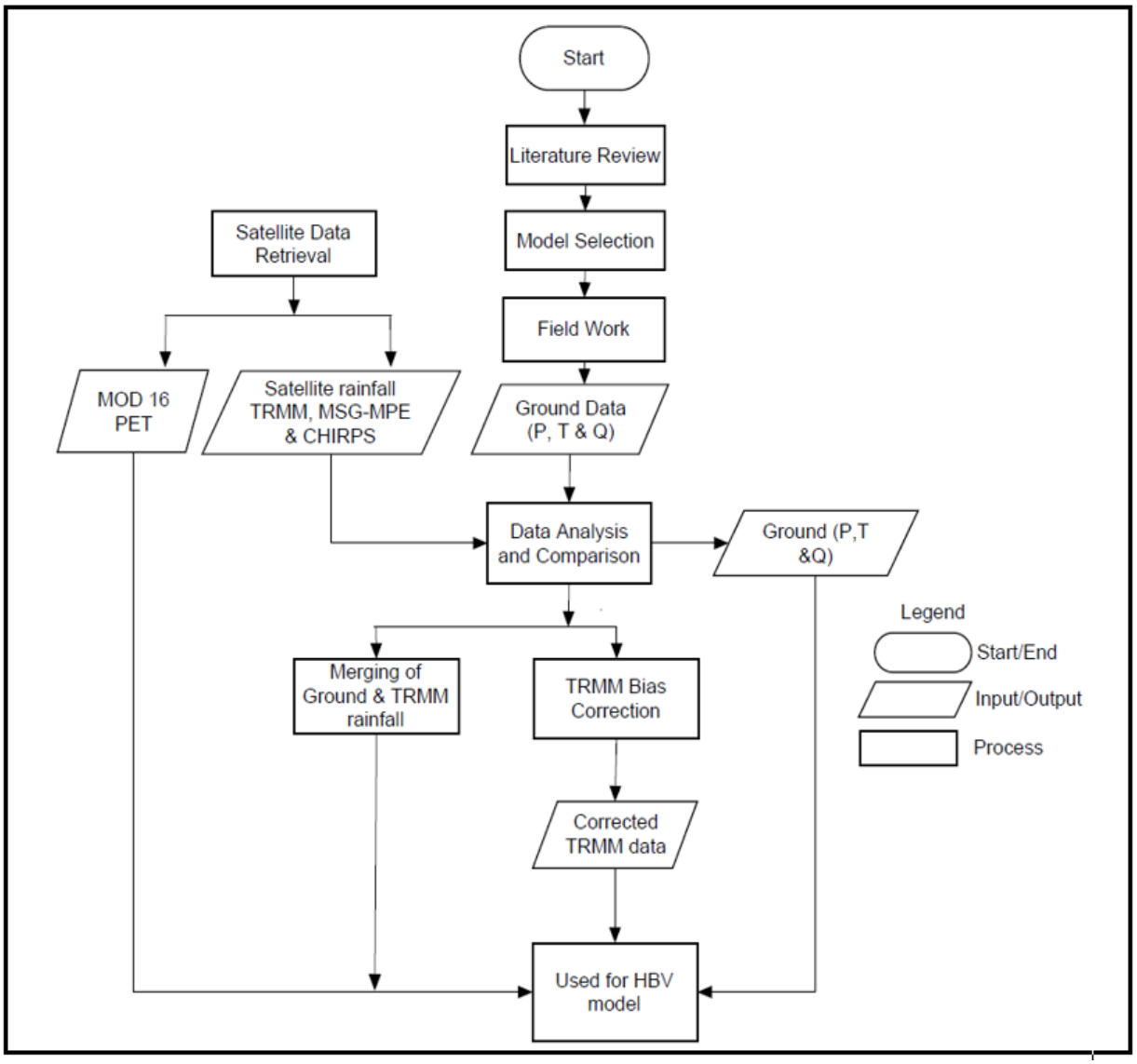

Figure 4.1: The adopted research methodology

4.1. Ground Data Analysis and Processing

i. Rainfall data analysis

Precipitation data were available for 18 rainfall stations located within/near the Kikuletwa sub-catchment. The time series dated back from 1950's to present even though there are gaps in most of the rainfall stations. As one of the objectives of this study is to compare the ground observed rainfall with satellite rainfall, a period of 2010-2014 was selected to match the available satellite data. Station records were screened and checked for records length, which resulted into six stations with full records as listed in Table 3.2 and plotted in Figure 3.1 above.

The consistency of rainfall data for the selected rainfall stations (2010-2014) was checked by double-mass curve method (Figure 4.2 and Appendix A). The method is a convenient way of checking the consistency of a record. It is a plot of cumulative data of a rainfall station against mean of the cumulative precipitation in a basin for the same period of time. The graphical plot has to be a straight line if there is a good correlation between the variables. A break in the slope of the line indicates an inconsistency of the data in the targeted station. This might be due to changes in the method of data collection or change in the physical condition of the catchment (Searcy & Hardison, 1960).

It can be observed from the plots that all the stations are consistent with a coefficient of determination (R^2 > 0.9). The slight shift of the curve might be due to meteorological events as the catchment is located in the mountainous area in which there is great variation of rainfall due to elevation. This brings variation of recorded rainfall even in the nearby stations. Since the observed breaks did not persist for more than five years, they can be ignored as they have no effect in the particular study (Searcy & Hardison, 1960).

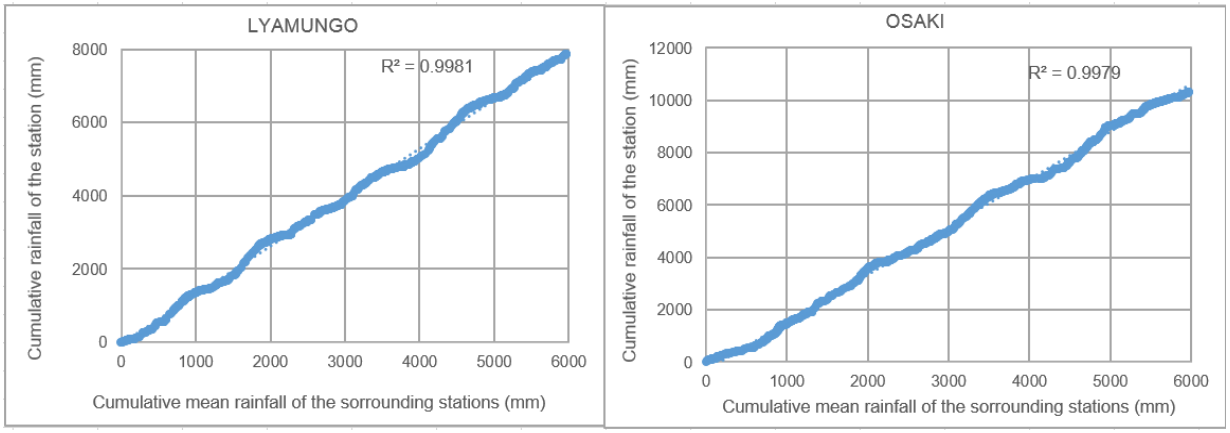

Figure 4.2: Rainfall station consistency check – Double Mass Curve

ii. Temperature data Analysis

Temperature data for 2010-2014 is available for three stations within the catchment. The stations are Kilimanjaro International Airport (KIA), Arusha Airport and Moshi Airport as indicated in Table 3.2.

iii. Estimation of catchment average aerial rainfall

The aerial average rainfall in the sub-catchment was calculated by using the Thiessen polygon method (Figure 4.3). It is a weighted mean method recommended in sub-catchments which meteorological variables are not uniform both in time and space (Bhavani, 2013). This is true in the Kikuletwa sub - catchment as rainfall varies from place to place and even their measuring stations are located only in the

upper part of the catchment. For that reason, estimation of spatial rainfall was necessary as the HBV Light model requires the representation of meteorological data in each sub-catchment. Thiessen polygon method assigns weight to each gauge station considering the proportion of the area contributing to that station to the total catchment area (Bhavani, 2013). The weighted meteorological variables were calculated by using the following equation.

$$K_w = \sum_{i=1}^{n} C_i * K_i \quad (4.1)$$

Where K_w is the estimated variable; C_i is the weight of the station; K_i is the measured variable in a particular station.

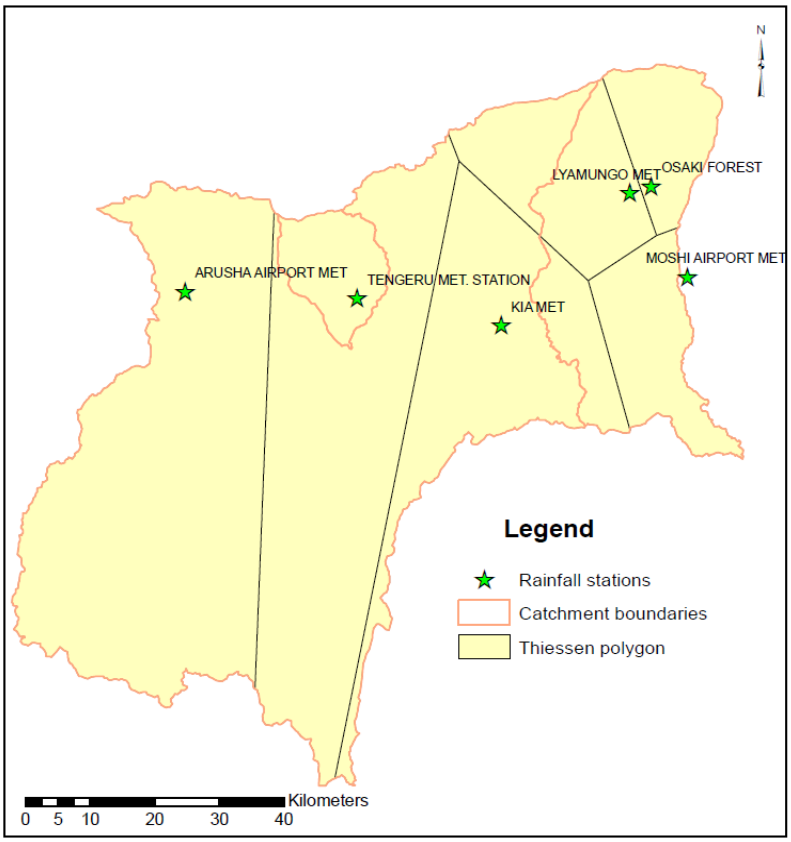

Figure 4.3: Areal representation of the catchment rainfall

iv. Discharge data

Discharge data from 2010-2014 for 1DD1 station (Table 3.1) have been analysed and gaps were observed from August to October, 2011. As the HBV Light model allows assigning -999 in case of missing discharge values, gaps in discharge data were not filled. The value -999 was assigned to all missing values before putting them into the model.

4.1.1. The Relationship between Rainfall and Discharge

The Runoff Coefficient (RC) method was used to characterise the relationship between rainfall and discharge in the catchment. RC explains the response of the catchment runoff to the fallen amount of rainfall. As physical conditions of the catchment are not similar, RC varies from one catchment to the other depending on their response to rain events and antecedent moisture. It is a large value (>2.5) for

areas with low infiltration example paved and steep slope areas while in permeable, well vegetated (forest) areas have low values (<2.5). The coefficient is calculated based on the equation 4.2 below as it is commonly assumed that, streamflow discharge is a percentage of rainfall depth (Katimon, Khairi, & Wahab, 2007). Quick discharge was obtained by separating the base-flow from the total discharge by using Time plot program (Arnold, Muttiah, Srinivasan, & M, 2000).

$$RC = \frac{Q}{R} \tag{4.2}$$

Where; RC is the runoff coefficient, R and Q are rainfall and quick discharge respectively both in (mm).

Furthermore, the relationship between rainfall and discharge was assessed by graphical plot as shown in Figure 4.4. Rainfall and discharge for 2010-2014 are plotted against time for the selected rainfall stations. It is clearly seen from the plot that the catchment responds to the rainfall as the major rainfall peaks are reflected in the hydrographs as major discharge peaks. On the other hand, during the period of low or no rainfall, most of the discharge is from the base flow.

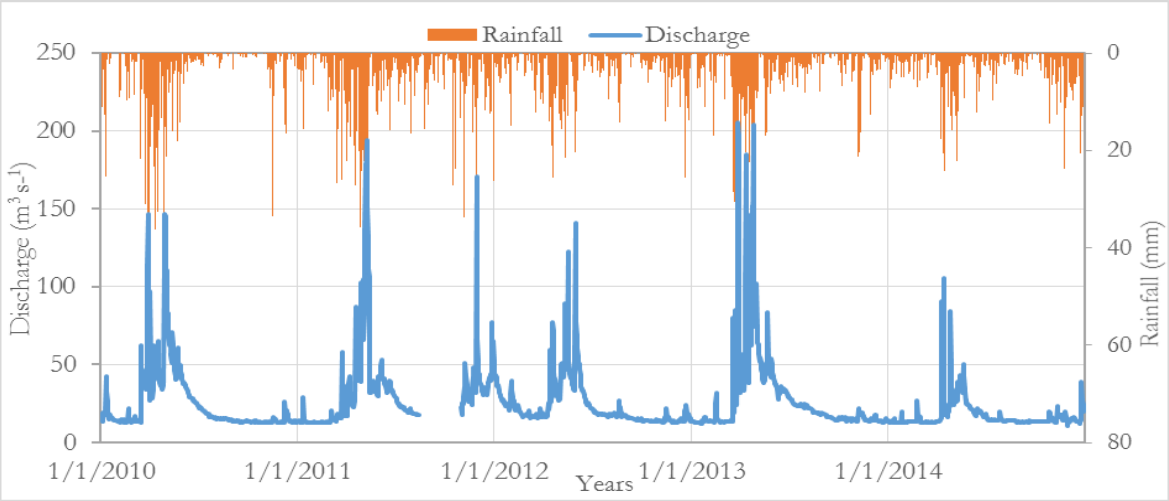

Figure 4.4: Relationship between Discharge and Rainfall

4.2. Satellite Data Retrieval, Processing and Analysis

4.2.1. Satellite Data Retrieval by In-situ and Online Data (ISOD)

ISOD Toolbox is a plugin software in Integrated Land and Water Information System (ILWIS) which was developed to enable online access of various environmental time series data and satellite images. It provides information about land surface variable such as precipitation, potential evapotranspiration, normalize difference vegetation indices, elevation information, weather and pressure forecast, which are useful in studying and monitor rapid changes on the earth's surface. The information obtained are of great importance, especially for developing countries where the gauge network are sparsely located or unavailable. The toolbox is an open source and it automatically retrieves and processes various data which are downloaded in different formats to an ILWIS format which is easy to use (B. Maathuis & Mannaerts, 2013). The ISOD Toolbox Structure is shown in Figure 4.5 below.

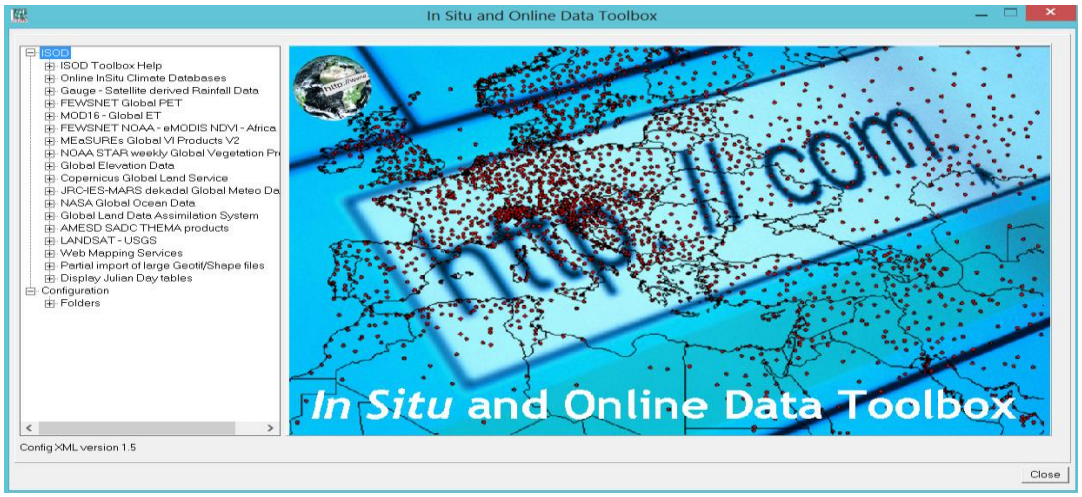

Figure 4.5: The ISOD Toolbox Structure (B. Maathuis & Mannaerts, 2013).

Daily satellite rainfall data and the 8 days PET have been retrieved from ISOD Toolbox in ILWIS. Batch file for each product was created to retrieve time series of data from 2010-2014. Also, a map-list of each product was created to facilitate the extraction of the rainfall and PET pixel values. At first, the satellite rainfall values were taken on the pixels which overlays gauge stations. Afterwards, the pixel values for the whole catchment were taken to enable sub-catchment rainfall comparison between satellite and ground rainfall. This was done by a cross function in ILWIS where by the catchment map was crossed with satellite images and an average daily value was obtained. The results of these procedures are shown (only for TRMM) in Figure 4.6. Since the potential evapotranspiration data set is available as a sum of the 8 days interval, its daily values were simply obtained by dividing each extracted value by eight.

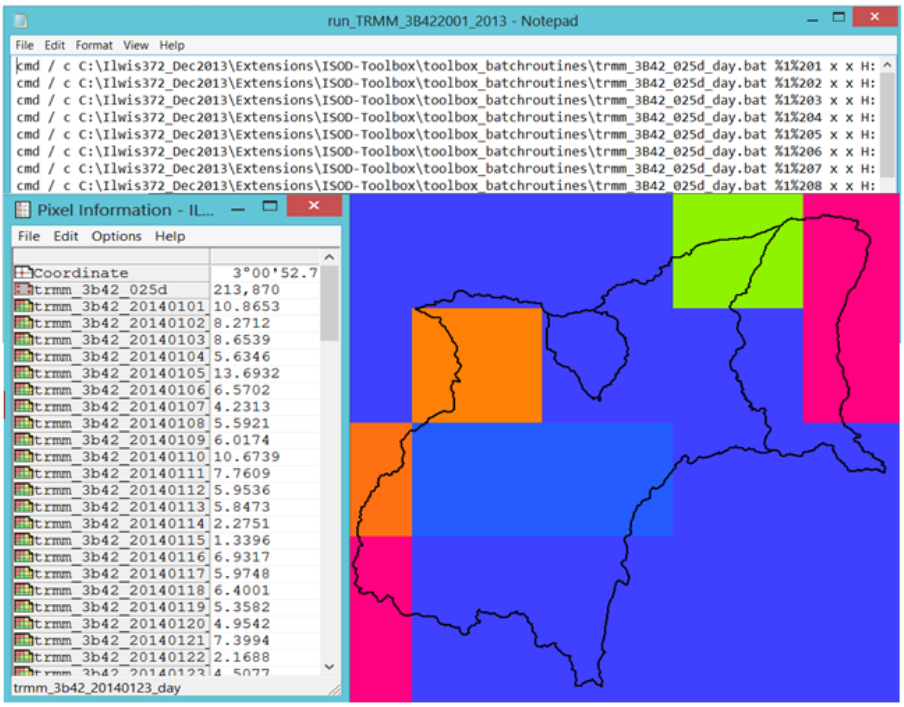

Figure 4.6: TRMM batch file and map-list for 2010-2014 (**Top**: the created batch file, **Bottom left:** rainfall values, **Bottom right:** catchment map overlaid on the TRMM map

4.2.2. Comparison of Satellite Rainfall Estimates with Ground Based Rainfall

Comparison of satellite rainfall estimates and ground observed rainfall has been done in two ways. Point to pixel comparison and an areal comparison for daily and monthly temporal scales.

In point to pixel method, a pixel value is compared with the ground station that overlays it. While in the areal comparison method, satellite estimates were compared with the interpolated ground rainfall station. This comparison is made at the sub-basin scale, meaning that the interpolated ground rainfall within sub-basin is compared with the average satellite rainfall estimates within the same sub-basin.

Evaluation of satellite rainfall products is of great importance since they suffer from some inherent shortcoming and have biases and random errors that are caused by various factors like sampling frequency, non-uniform field of view of the sensors and uncertainties in the rainfall retrieval algorithms. It is therefore essential to validate them with conventional rain estimates (Li, Zhang, & Xu, 2013). For these reasons, Haile et al. (2013) suggests different statistical methods to evaluate the reliability and accuracy of satellite rainfall data. Moreover, the capability of satellite rainfall products to detect rainfall has been accessed.

4.2.3. Statistical Analysis

Statistical methods are used to relate existing relationship between two data sets. The following methods have been selected for this study, they include measures of systematic differences (e.g. bias or mean difference aggregated over the entire seasonal sample), root mean square error (RMSE) and correlation coefficient (R).

The RMSE measures the average magnitude of the error between satellite rainfall estimates and ground based rainfall. Its value ranges from 0 to ∞, with lower values indicating an ability of satellite rainfall estimates to represent the observed ground rainfall measurements. The RMSE is expressed as;

$$RMSE = \sqrt{\frac{\sum_{i=1}^{n}(R_S - R_G)^2}{n}} \tag{4.3}$$

Correlation coefficient measures the strength of association between two data sets, here satellite and ground rainfall. It varies from -1 to 1, in which -1 indicates perfect negative correlation, 0 indicate that there is no correlation while 1 indicate there is perfect positive correlation. Its equation reads:

$$R = \frac{\sum_{i=1}^{n}(R_S - \bar{R}_S)(R_G - \bar{R}_G)}{\sqrt{\sum_{i=1}^{n}(R_S - \bar{R}_S)^2}\sqrt{\sum_{i=1}^{n}(R_G - \bar{R}_G)^2}} \tag{4.4}$$

Mean difference (MD) measures systematic difference between the estimated satellite and ground rainfall accumulated over the entire study period. Perfect value for MD is 0 meaning that, the amount of rainfall observed is the same as the estimated rainfall. It is expressed as;

$$MD = (\sum_{i=1}^{n} R_S - \sum_{i=1}^{n} R_G)/n \tag{4.5}$$

Total Bias (B) is the difference between estimated rainfall and the observed rainfall over the entire study period.

$$B = \sum_{i=1}^{n} R_S - \sum_{i=1}^{n} R_G \tag{4.6}$$

Where R_S and R_G are satellite and gauge rainfall intensities, respectively, the over bar symbol denotes the sample mean and n represents the number of samples.

4.2.4. Bias Observation, Decomposition and Correction

To evaluate the consistency of TRMM, CHIRPS and MSG-MPE rainfall estimates with ground measurements, a cumulative mass curve was plotted (Figure 5.4 and 5.5). However, it was observed that all satellite rainfall estimate (SRE) products systematically underestimated the observed rainfall. This is because satellite data are associated with systematic (bias) and random errors which need to be refined and corrected before being used for hydrological application (Li et al., 2013). Bias calculated in equation 4.6 above gives only the total bias of satellite rainfall estimates and ground observation over the entire sample without specifying the source of such differences. Therefore, in order to understand the different sources of bias, it is advised to break the total bias into three categories, namely hit bias, missed rainfall bias and false rainfall bias.

i. **Hit bias** occurs when both satellite and gauge record rainfall,

ii. **Missed rainfall bias** occurs when gauge record rainfall but satellite did not record rainfall and

iii. **False rainfall bias** is when satellite record rainfall but not recorded by the gauge (Habib, Larson, & Graschel, 2009).

The decomposed biases are mathematically expressed as;

$$\textbf{Hit Bias} = \sum(R_S - R_G)\ (when\ R_S > 0\ and\ R_G > 0) \quad (4.7)$$

$$\textbf{Missed Rainfall Bias} = \sum R_G\ (when\ R_S = 0\ and\ R_G > 0) \quad (4.8)$$

$$\textbf{False Rainfall Bias} = \sum R_S\ (when\ R_S > 0\ and\ R_G = 0) \quad (4.9)$$

Where R_S and R_G are satellite and gauge rainfall respectively, and both bias components are expressed in millimetres (Habib et al., 2009).

4.2.5. Bias Correction

In order to improve satellite rainfall estimates from the observed bias, bias correction method was applied to daily satellite rainfall values. The correction methodology is based on Cumulative Distribution Function (CDF)-matching technique. CDF-matching technique mainly focuses on the adjustment of satellite rainfall distribution within the catchment. By so doing, it allows the correction of different sources of error in the satellite rainfall. Thus, the bias corrected satellite estimates can be applied for hydrological and environmental studies (Müller & Thompson, 2013). Equation 4.10 adopted from Piani et al., (2010) was used to correct satellite rainfall estimates.

$$Satellite_{corrected} = (a + bx)\left(1 - e^{(-(x-x0)/\tau)}\right) \quad (4.10)$$

Where, a, b and τ are calibration parameters, x is the rainfall to be corrected and x_0 is the dry day correction term.

4.2.6. Detection Capability

The performance of TRMM, CHIRPS and MSG-MPE in detecting rainfall has been assessed by three categorical statistics, namely Frequency Bias Index (FBI), Probability of Detection (POD) and False alarm Ratio (FAR). They are calculated based on a 2 x 2 contingency table (Table 4.1) and the rainfall threshold of 0.5 mm day^{-1} (Abiola, Mohd-mokhtar, Ismail, Mohamad, & Mandeep, 2013).

Table 4.1: Contingency table

		Ground Rainfall (gauge)	
		Rain	No-rain
TRMM-3B42 estimated rainfall	Rain	Hit	False alarm
	No-rain	Misses	Null

Where;

- Hit - rainfall events correctly detected by the satellite,
- Missed - rainfall events observed by the gauge but not detected by the satellite,
- False alarms - rainfall events detected by the satellite but not observed by the gauge and
- Null - rainfall events neither observed by the gauge nor detected by the satellite.

The POD measures the fraction of rain events that were correctly detected by SRE.

The FBI analysis gives the ratio of the satellite rainfall estimates to the actual precipitation events.

The FAR measures the fraction of false alarms in the satellite estimates.

POD, FAR values ranges from 0 to 1, with 1 being the perfect score for POD and 0 is the perfect score for FAR. Values for FBI ranges from 0 to ∞ with the perfect score being 1 (Abiola et al., 2013). They are expressed as follows;

$$POD = \frac{Hit}{Hit + Misses} \tag{4.11}$$

$$FAR = \frac{False\ Alarm}{Hit + False\ Alarm} \tag{4.12}$$

$$FBI = \frac{Hit + False\ Alarm}{Hit + Misses} \tag{4.13}$$

4.2.7. Merging of Satellite and Ground Rainfall Data

Merging rainfall datasets from different rainfall sources has been proved to improve rainfall estimates from satellite, because it take advantage of both techniques to produce more accurate and reliable data. Even though satellite rainfall data act as an alternative to the ground observation due to its high spatial and temporal resolution, they suffer from poor detection capabilities in some of the areas, false detection and bias (Tobin & Bennett, 2010). This study will try to merge rainfall from satellite (TRMM) and ground rainfall in order to remove biases from satellite data and to create good relationship with ground rainfall, also to produce an acceptable rainfall data for streamflow simulation.

To accomplish this task, a filter based on the utilisation of the actual ground rainfall data was developed. First, all dates with missing data were omitted, then dates in which satellite product did not record rainfall were adjusted through substitution of ground rainfall data (Tobin & Bennett, 2010). The adjusted satellite data were later corrected based on section 4.2.5. After correction, the data were used as input to the model.

4.3. Hydrological Modelling

Response routine with *delay model structure* was used to simulate discharge within the catchment. The structure is suitable for catchments with deep groundwater (Jan Seibert, 2005), as it is the case for Kikuletwa catchment. Unlike the standard model structure, where the whole amount of water from the soil moisture zone goes to recharge the upper zone storage and then to the lower zone storage through percolation, in this structure the recharge coming from the soil zone is divided into two parts. The first part is directly added to the lower zone and the remaining part is evenly distributed in the upper zone storage as illustrated in Figure 4.7 (Jan Seibert, 2005). Moreover, the steps outlined in Figure 4.8 were followed in the modelling process.

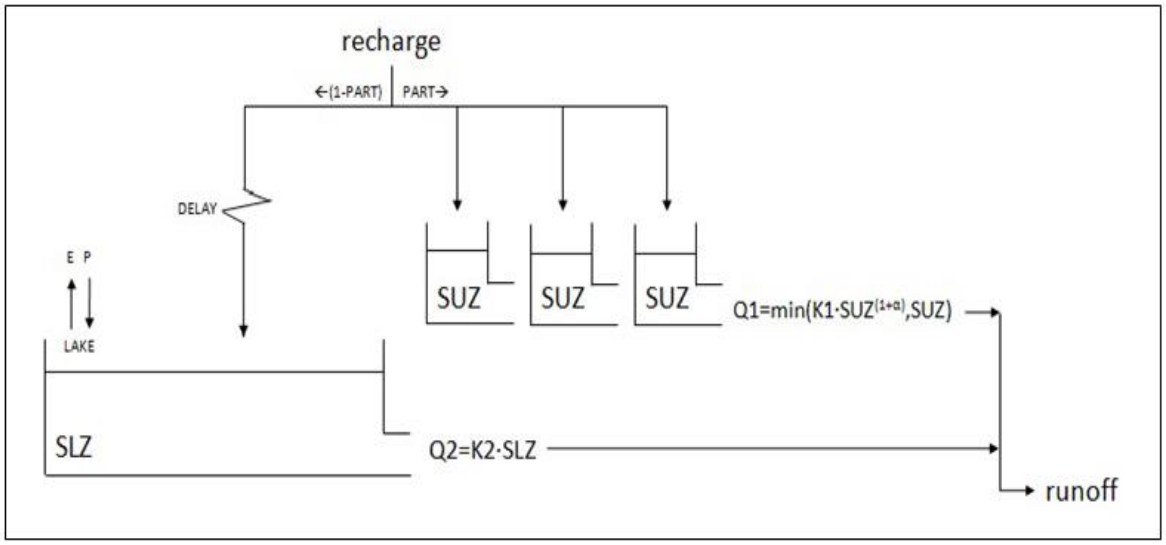

Figure 4.7: Response routine with delay model structure

Where:

- Recharge is the water input from soil routine (mm/Δt),
- SUZ and SLZ are upper and lower zone storages respectively (mm),
- E – Evaporation from the lake,
- P - Precipitation to the lake,
- K1 and K2 are recession coefficients (l/Δt),
- QI and Q2 are discharges from upper and lower zone respectively.
- PART – is the portion of recharge added to the upper zone storage while;
- DELAY is the period of delay for water added to the lower zone storage (Δt).

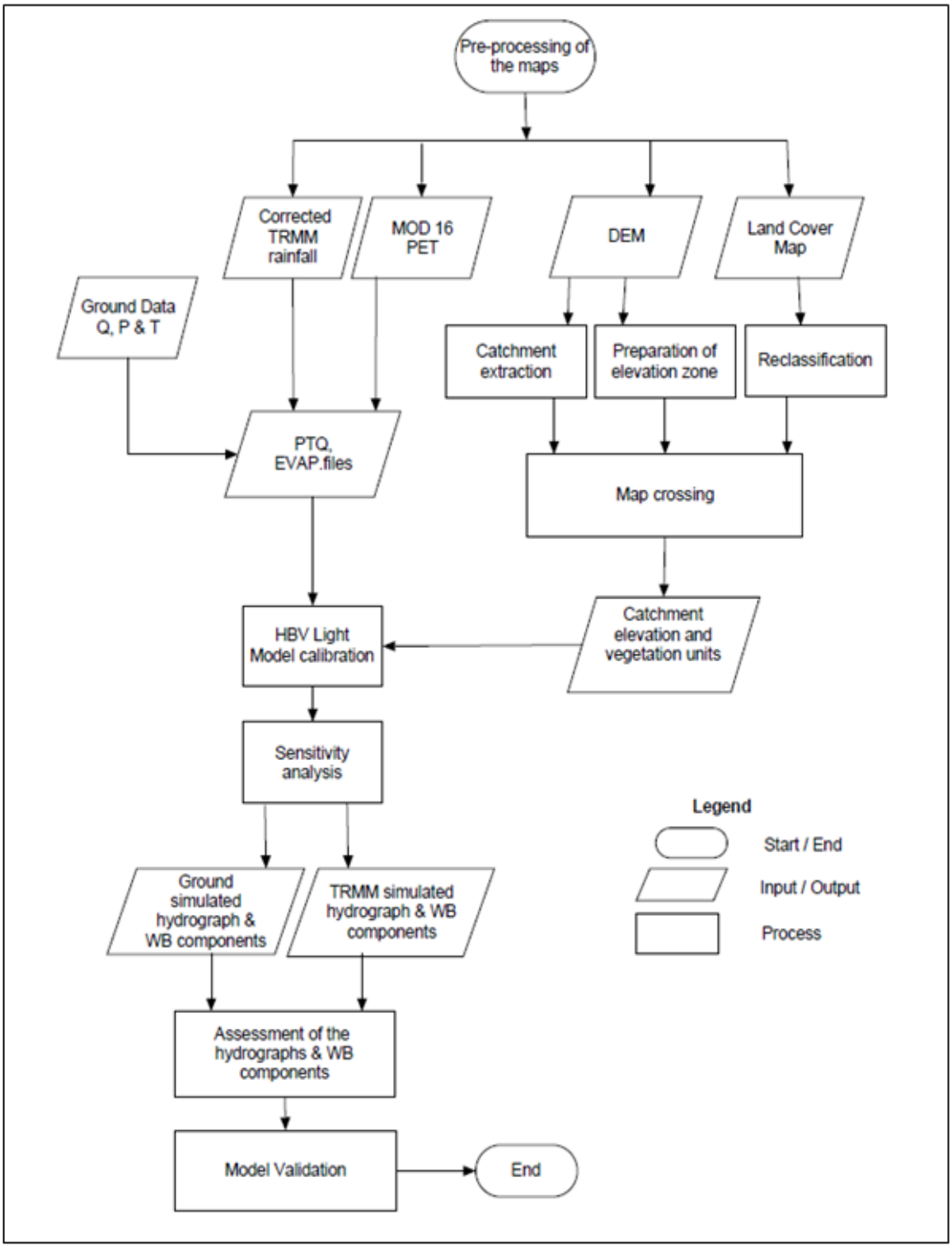

Figure 4.8: Steps followed during hydrological modelling

4.3.1. Model Setup

a) Catchment extraction

Kikuletwa sub-catchments map was delineated from a 90m Digital Elevation Model (DEM) from Shuttle Radar Topographic Mission (SRTM). The DEM was downloaded from SRTM website and imported to ArcMap for processing. Since the DEM has cells that does not have a defined drainage value, a fill sink operation was performed to remove any sink through interpolation technique (B. H. P. Maathuis & Wang, 2006). Thereafter, flow direction and flow accumulation were determined with a threshold number of pixels = 5000 assigned during catchment extraction. The catchment was divided into three sub-catchments considering the places where there is a discharge station.

b) Preparation of Elevation Zones

The Shuttle Radar Topographic Mission (SRTM) digital elevation model of 90m spatial resolution was used to determine elevation ranges within the sub- catchments. The sub-catchment elevation varies from 683 to 5875 m-asl, which allows the slicing of the DEM into 19 elevation zones of 300 m intervals. Slicing of the DEM allows the model to take into account the effects of slope and differences in temperature in each zone during runoff simulation (J. Seibert & Vis, 2012). Figure 4.9 below shows the generated elevation zones.

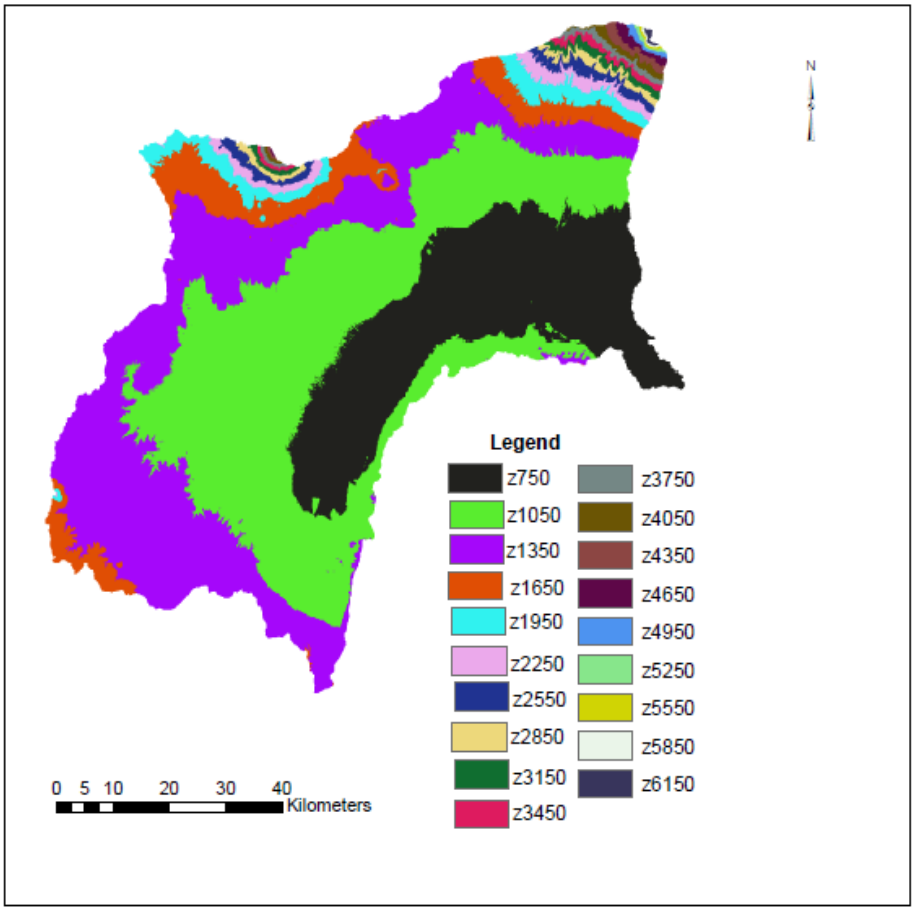

Figure 4.9: Sliced elevation zones

c) Preparation of Vegetation Zones

Kikuletwa land cover map was extracted from Tanzania Land cover map of 2010. The map has the following units; natural forest, grasslands, bush lands, cultivated land, built up areas, bare soil, woodland, springs and swampy areas. As HBV model requires the maximum of three land covers units, the original land cover map was rasterized and re-classified into three units namely, Forest, Cropland and Built-up areas. It also allows the inclusion of lakes present in the catchment. The re-classified land cover map is presented in Figure 4.10 with forest covering 49 %, cropland covering 46 %, lakes covering 4.4 % and built up areas covering 0.6 %.

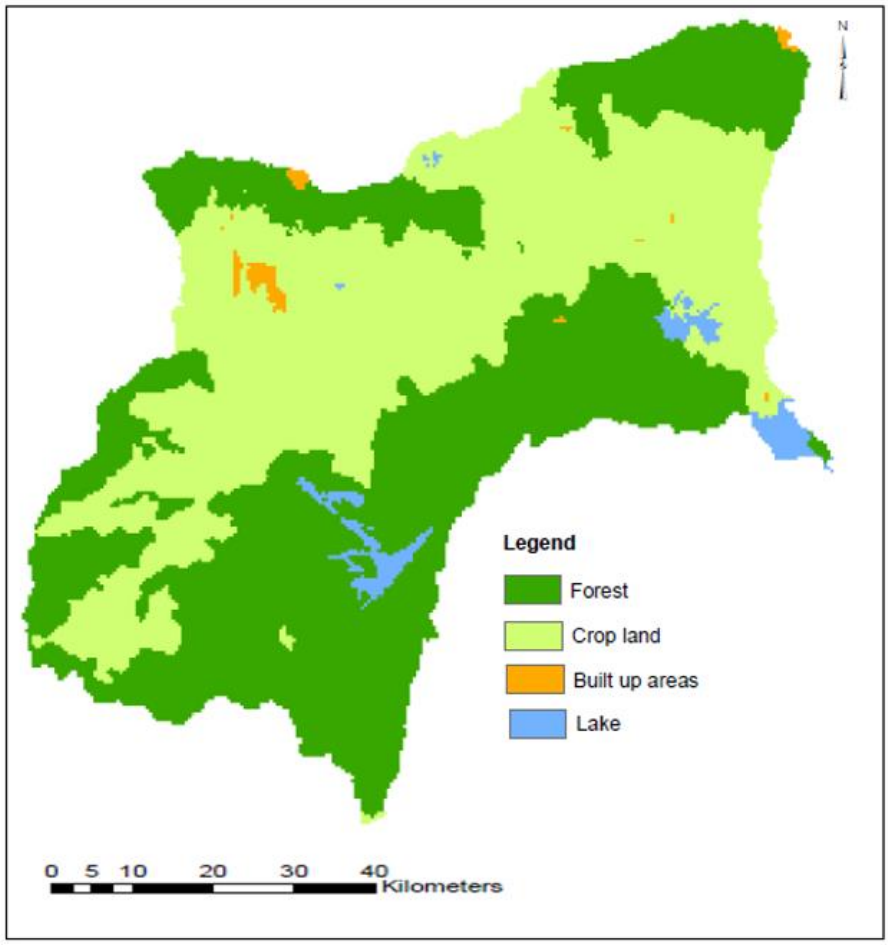

Figure 4.10: Reclassified land cover units

d) Preparation of Hydro-meteorological data

In order to set up HBV-Light model the following files are required, Precipitation-Temperature-Discharge (PTQ), Evaporation and Sub-Catchment files. The PTQ file contains time series of daily rainfall (mm day^{-1}), temperature (^{0}C) and discharge (mm day^{-1}). While, an evaporation file contains potential evapotranspiration values in mm day^{-1} (Jan Seibert, 2005).

In this study, an interpolated ground rainfall and an estimated rainfall from TRMM based on sub-basin scale were used in creating the file together with the temperature data. Discharge data were converted from m^3 s^{-1} to mm day^{-1} by dividing with the catchment area. The evaporation file contains 365 daily mean values from MOD 16 was also prepared.

Sub-Catchment file which describes the spatial relation between sub-catchments (i.e. flow of water from upper sub-catchments to an outlet) was also created. On the other hand, the physical characteristics of the catchment based on elevation-vegetation zones and lakes were prepared and fed into the model.

4.3.2. Model Calibration and Sensitivity Analysis

Model Calibration

The model has been calibrated with ground and satellite rainfall data for the period of 2011-2013. As the model calibration entails the modification of parameter values and comparison of the predicted output of interest to measured data (Ababa, 2011), the model has been calibrated independently for the four datasets until an adequate threshold for the objective function is achieved.

In this study, a time series of 2010 has been used in warming up the model. Model calibration was done manually by trial and error method through changing one parameter at a time. The parameters in each zone (soil moisture, upper and lower zones) were tuned to represent the real catchment characteristics. Those parameters are; field capacity (FC), Limit for potential evapotranspiration (LP), Beta (β), Alpha (α), Recession coefficients (KI and K2), MAXB, PART and DELAY. Model calibration was performed until a satisfactory fit of the simulated hydrograph was observed. In order to improve the results, a sensitivity analysis was performed and the sensitive parameters were calibrated until the simulated discharge nearly matches the observed discharge. The calibration was stopped when there was no improvement of the model results on parameter change. This process resulted in an optimized parameter set that represents the catchment, simulated hydrographs and water balance components. After calibration, the water balance components together with the timing of the discharge peaks and the distribution of the base-flow of the simulated discharge have been compared and analysed.

The results of calibration should be evaluated both qualitatively and quantitatively in order to see the predictive capability of the model. According to Rientjes (2014), there are several objective functions which are widely used in assessing the performance of surface water models. They include Nash-Sutcliffe coefficient of efficiency (NS) and Relative Volumetric Error (RV_E). In this study both objective functions (Table 4.2) have been used to assess the fit of simulated discharge to observed discharge.

Table 4.2: Objective functions

Objective Functions	Value Ranges	Perfect Value
$NS = 1 - \frac{\sum_{i=1}^{n}\left(Q_{obs(i)} - Q_{sim(i)}\right)^2}{\sum_{i=1}^{n}\left(Q_{obs(i)} - \overline{Q_{obs}}\right)^2}$	$-\infty$ to 1	1
$RV_E = \left(\frac{\sum_{i=1}^{n} Q_{sim(i)} - \sum_{i=1}^{n} Q_{obs(i)}}{\sum_{i=1}^{n} Q_{obs(i)}}\right) * 100$	$-\infty$ to ∞	0

Where: Q_{obs} and Q_{sim} are observed and simulated discharge respectively.

Sensitivity Analysis

Sensitivity analysis is performed to see how much model output values are affected by changes in the model input parameters. If the model output value changes highly with a slight adjustment of parameter values, then we can say that the model is sensitive to that parameter, while if the model does not respond

much even with the larger change of the input parameters we concluded that the model is insensitive to the respective parameter (Ouyang, Puhlmann, Wang, von Wilpert, & Sun, 2014). For this study, sensitivity analysis was first performed when fitting the baseflow followed by the peak flow.

4.3.3. Model Validation

The best way of assessing the reliability of a calibrated model is through validation procedure. The Model needs to be tested for its accuracy and reliability because, sometimes the model cannot well represent the real world systems due to errors in model structure and the observed variables which brings model uncertainty. Therefore, the validity of the model is assessed against a second independent set of stress condition (M. Rientjes, 2014). For this study, the time series of 2014 has been used for validation.

5. RESULTS AND DISCUSSION

5.1. Rainfall Data Analysis

Monthly average rainfall plotted in Figure 5.1 depicted a bimodal rainfall pattern with an approximately 61% of the annual rainfall occurring between March – May and 29% of the rainfall occurring in November and December. However, annual average rainfall between stations varies from 490 and 2029 mm yr^{-1} from 2010-2014 and an increase of rainfall is observed with an increase in elevation as the station with annual average rainfall of 490 mm yr^{-1} is located at 891 m while the station with annual average rainfall of 2029 mm yr^{-1} is located at 1344 m.

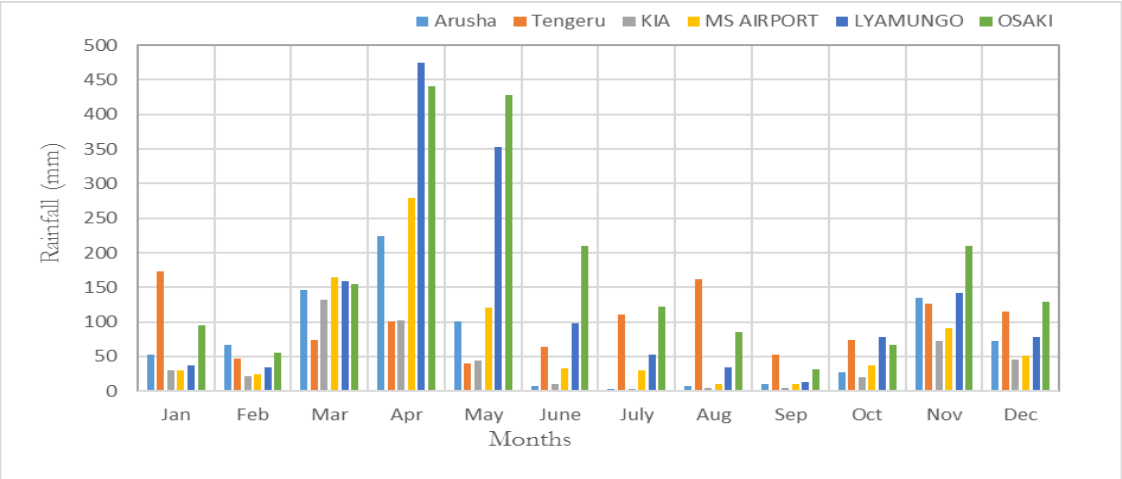

Figure 5.1: Average monthly gauge rainfall distribution (2010-2014)

5.2. Relationship Between Rainfall And Discharge

The Runoff Coefficient (RC) was used to assess the relationship between rainfall and discharge which is generated in the catchment. The analysis based on section (4.1.1) which explained about establishing the existence relationship between amounts of rainfall occurs within the catchment and how much rainfall is transformed into runoff. It is a simple way to visualize the behavioural change of a catchment for a certain period of time. The seasonal RC values plotted in Figure 5.2 shows a slight variation during the study period. Generally, the variation of RC values can be due to several factors which lead to changes in catchment characteristics hence affects runoff. One of the factors could be due to changes in land use and land cover in the catchment (Katimon et al., 2007). For this particular season (rainy season March-May), it was observed that there is a relationship between rainfall depth and RC values (Table 5.1). An increase of rainfall causes the RC values to increase because, when the precipitation amount is larger, more water will be converted to runoff as saturated area increases during the rainfall process. Likewise, when amount of rainfall is small, little amount of water will be converted to runoff as a lot of water will be needed to fill up the soil before leaving the catchment and hence low RC values (Feng & Li, 2008).

Note: Quick discharge was obtained after separating the base-flow from the total runoff (Appendix C – only for 2010).

Table 5.1: Seasonal relationship between rainfall and runoff coefficient (March-May)

Years	R (mm)	Q (mm)	RC
2010	683.31	17.82	0.026
2011	594.60	17.52	0.029
2012	342.45	9.36	0.025
2013	561.00	23.00	0.041
2014	289.74	6.19	0.020

Figure 5.2 below, shows that the amount of satellite estimated rainfall is too small as compared to the amount of discharge produced within the catchment. For example, in the highest peak 200 m^3s^{-1} (March – May, 2013) the amount of satellite estimated rainfall was approximately 20 mm. This is because both satellite products underestimated the amount of rainfall in the area. On the other hand, in January 2014 for instance MSG-MPE has much rainfall, which is not well reflected in discharge also in March, 2014 for CHIRPS. This is because of the false rainfall events recorded by those satellites.

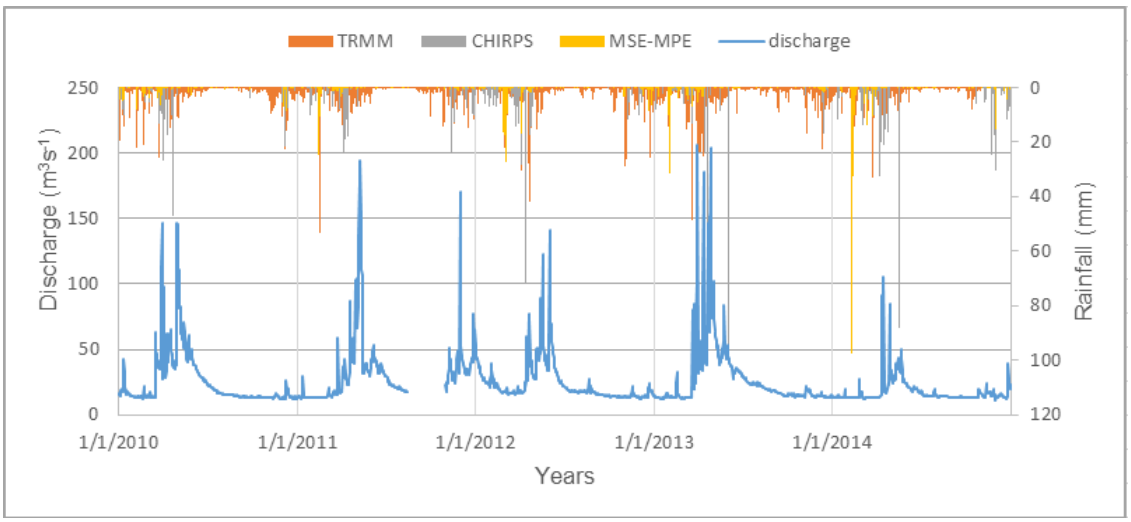

Figure 5.2: Relationship between satellites estimated rainfall and discharge

5.3. Comparison of Satellite Rainfall Estimates with Ground Based Rainfall

5.3.1. Point to Pixel Comparison

The pixel of satellite rainfall estimation (TRMM, MSG-MPE and CHIRPS) has been compared with a ground rainfall station within that pixel to see their relationship. The comparison is based on graphical plots and a statistical analysis (section 4.2.4). Firstly, the mean annual rainfall for ground and satellite rainfall estimates is plotted in Figure 5.3 in each station to see the ability of these products to capture the amount of rainfall falling in the catchment. It is observed that all satellite rainfall products underestimated the amount of rainfall in all stations but TRMM shows better figures and a higher correlation with ground rainfall. Those differences are also seen on the cumulative plots (Figure 5.4 and 5.5). The deviation of satellite cumulative curves from the ground cumulative curve indicates that there are some errors associated with SRE products which hinder their performance. These errors can be due to the type of algorithms which are sensitive to one type of precipitation and less sensitive to others and inability to capture short rainfall (Müller & Thompson, 2013).

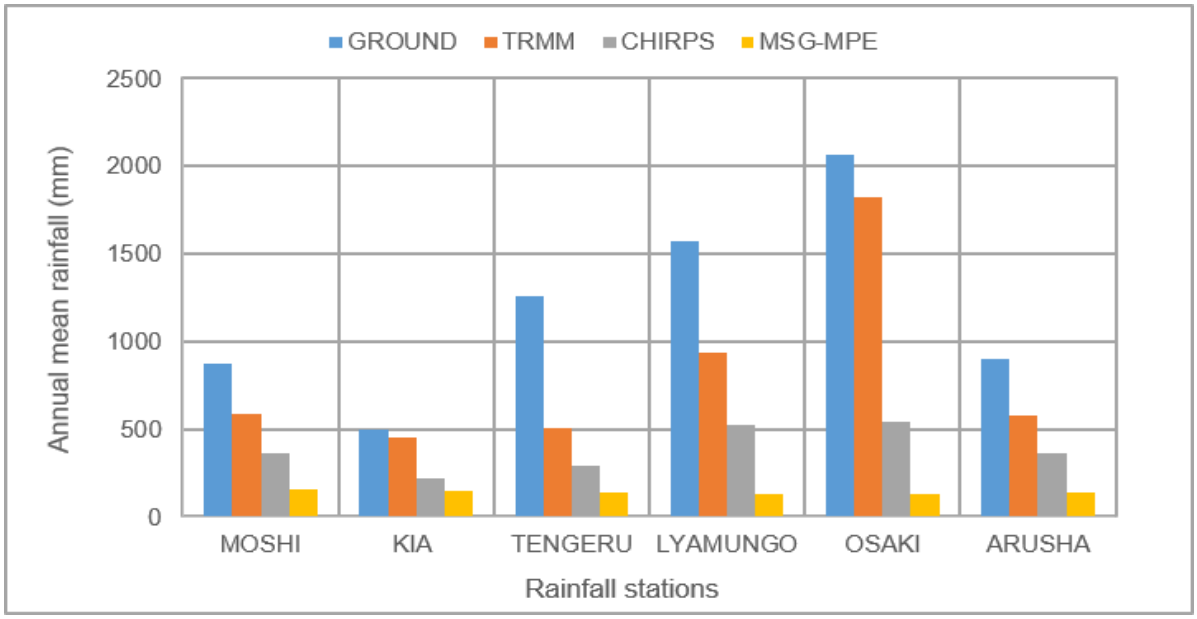

Figure 5.3: Comparison of annual mean rainfall for Ground, TRMM, MSG-MPE and CHIRPS

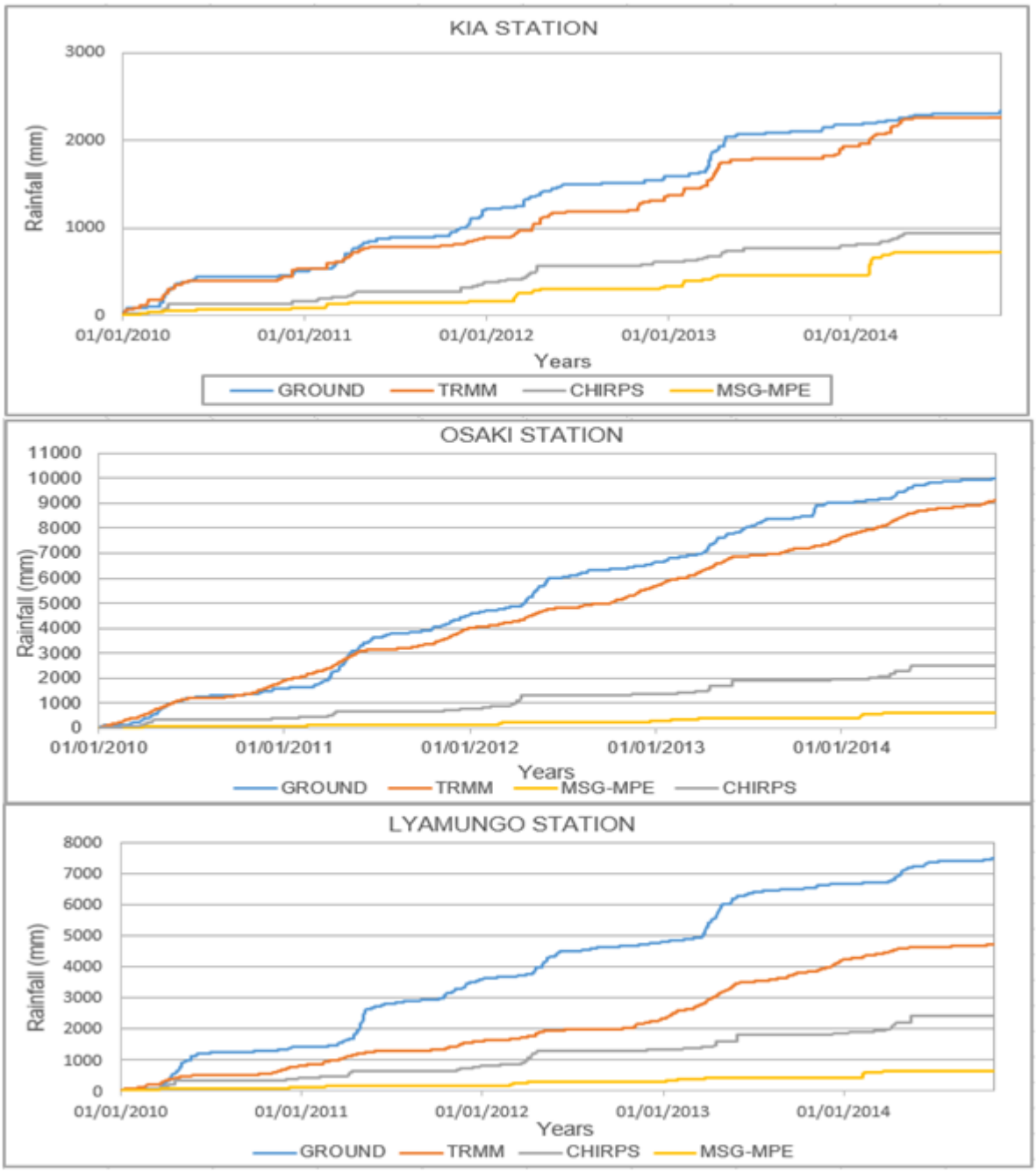

Figure 5.4: Cumulative mass curve for GROUND, TRMM, CHIRPS and MSG-MPE rainfall

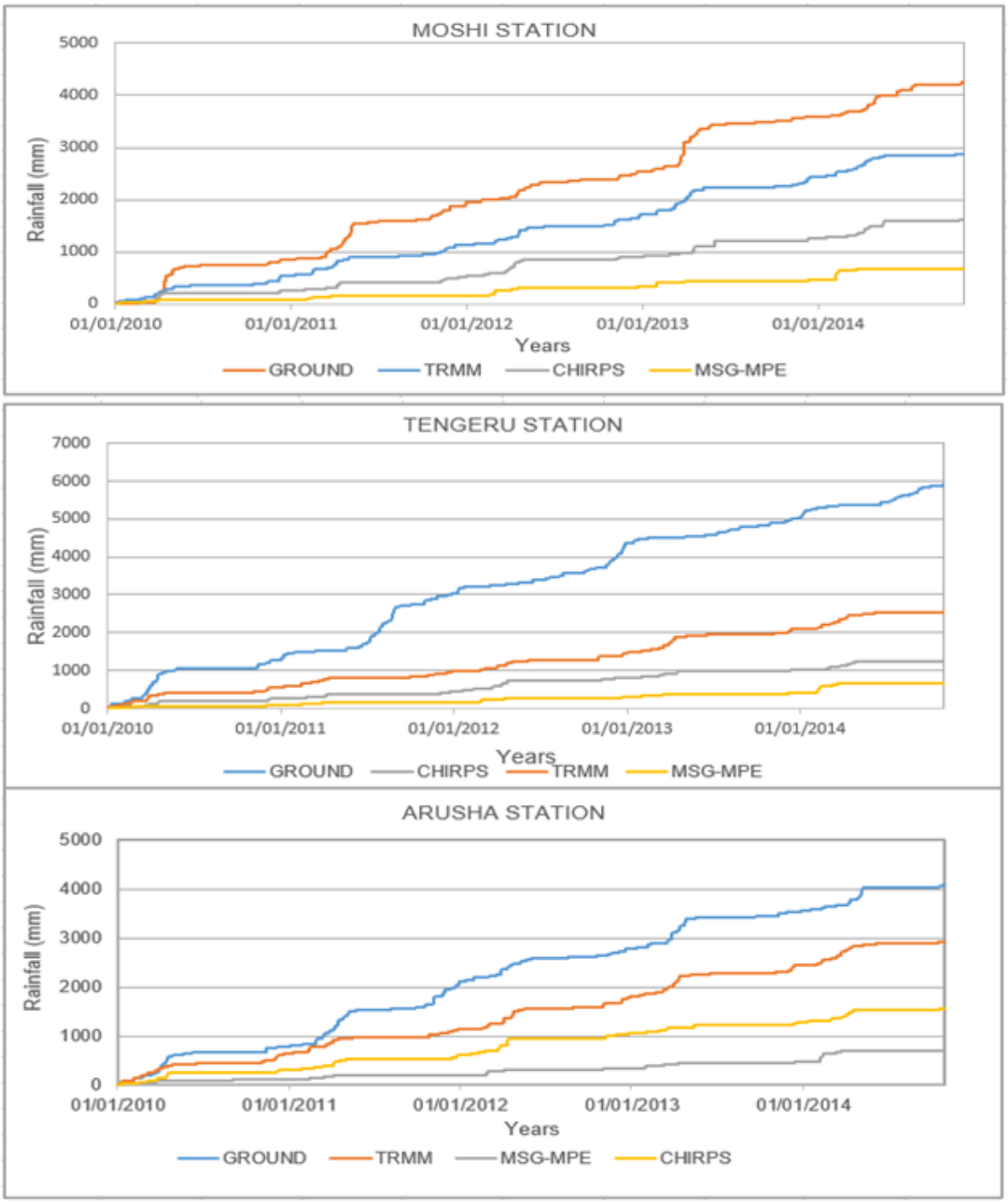

Figure 5.5: Cumulative mass curve for GROUND, TRMM, CHIRPS and MSG-MPE rainfall

Temporal distribution of rainfall was also assessed and it has been found that rainfall estimates from TRMM agrees with the ground based rainfall for about 64% of the annual rainfall that occurs in heavy rain season from March –May, as illustrated in Figure 5.6. Contrarily, CHIRPS captures only 35% while MSG-MPE was able to capture only 6% of rainfall during rainy season. Monthly rainfall for satellite products was obtained by summing rain values which are available in that month (dates with missing values were ignored). Moreover, both TRMM and CHIRPS satellite data were able to depict the bimodal rainfall

pattern within the study area which is not the case for MSG-MPE satellite as it can be observed in the plot below.

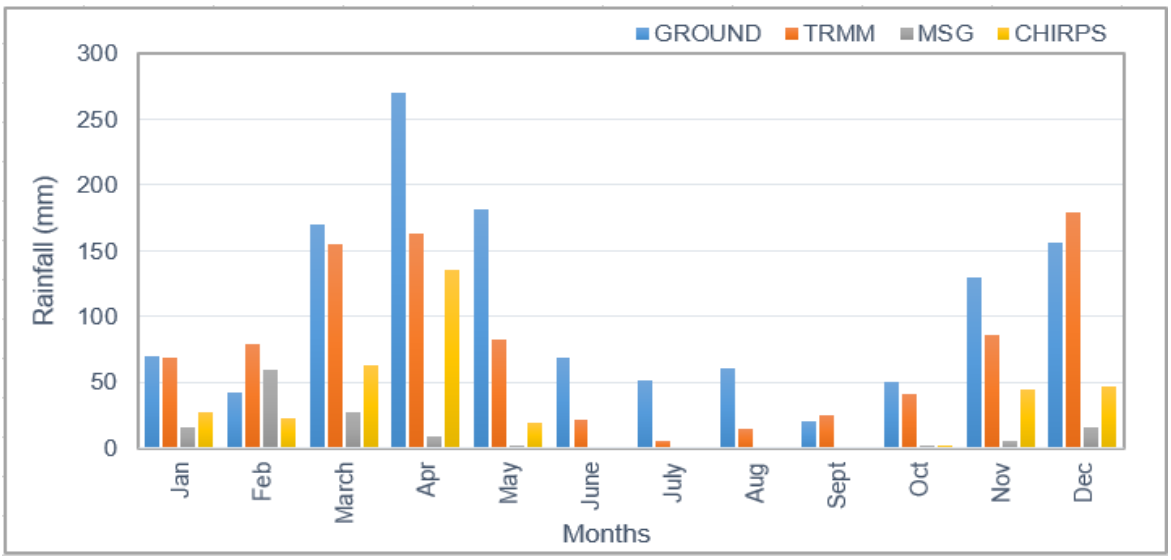

Figure 5.6: Temporal distribution of rainfall

Daily correlation coefficient (R) analysis indicated that the satellites were not able to represent the amount of rainfall in the catchment. However, since TRMM data has been adjusted to gauge rainfall in monthly scales (Huffman et al., 2007b), a monthly comparison of satellite and ground rainfall data was also performed. Firstly, all dates with missing values were omitted and both ground and satellite rainfall data were aggregated to monthly temporal intervals. The monthly comparison resulted in a good correlation coefficient (Figure 5.8, 5.8 and 5.9) because, most of the biases which are associated with the inconsistency of observation data or missing of satellite data have been minimised. As a result, TRMM shows a better correlation (Figure 5.8) with R ranging from 0.5 to 0.7 indicating a better fit with ground rainfall data and was therefore selected for use in the HBV-Light model simulation. The monthly correlation coefficients of CHIRPS and MSG-MPEG were ranging from 0.4 to 0.5 and 0.3 to 0.4 respectively (Figure 5.7 and 5.9). The TRMM RMSE ranges between 6.7 to 12 mm day^{-1}, while MSG-MPE and CHIRPS data ranges between 11 to 19 mm day^{-1} and 6 to 16 mm day^{-1} respectively. The negative Mean Difference (MD) ranging from -0.77 to -0.02 for TRMM, -2.2 to 0.29 for MSG-MPE and -4.2 to -0.8 for CHIRPS is also an indication of an underestimation of rainfall in most of the stations, except KIA station in which there is an overestimation of 0.29 mm by MSG-MPE.

The results are similar to those of Dinku et al., (2007) who found that the TRMM tends to underestimate occurrences and the amount of rainfall in the complex orographic terrain of Africa due to its associated warm rain process. Moreover, Worqlul et al., (2014) showed that MPEG is constantly under depicting the observed rainfall due to its algorithm which is much more suitable for convective rainfall.

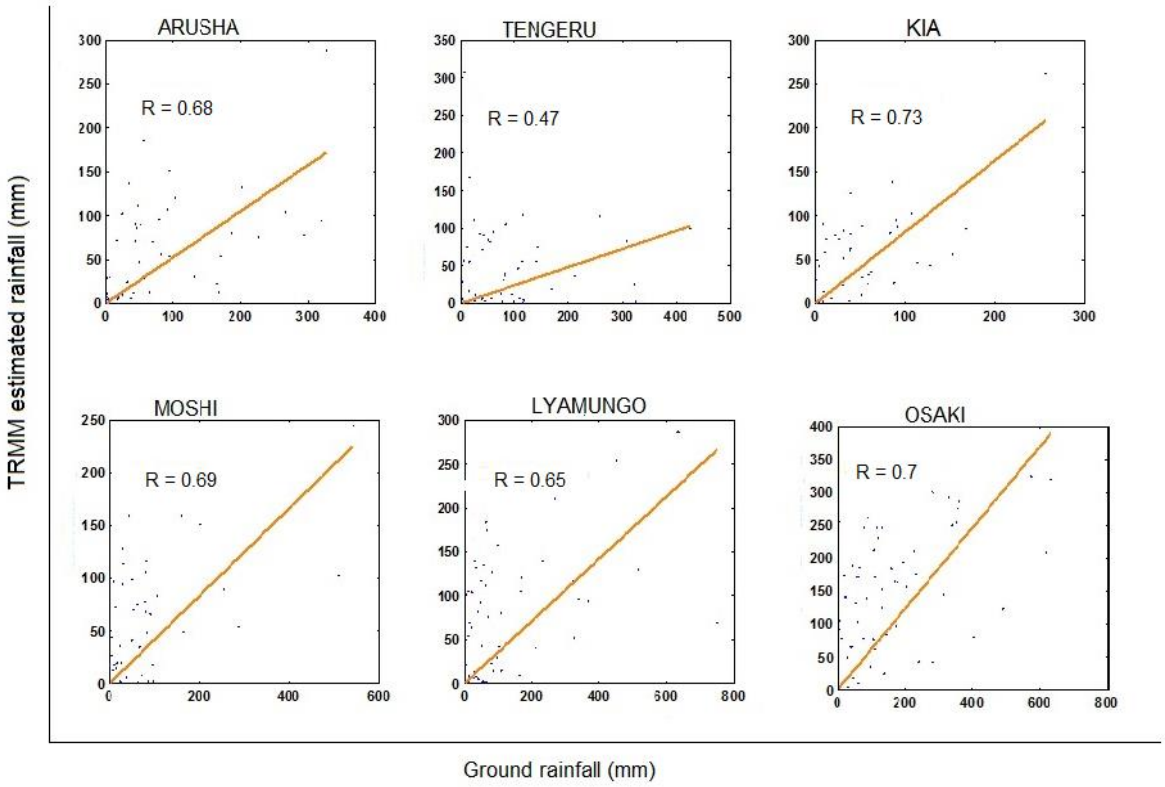

Figure 5.8: Monthly correlation between TRMM estimated rainfall and ground rainfall

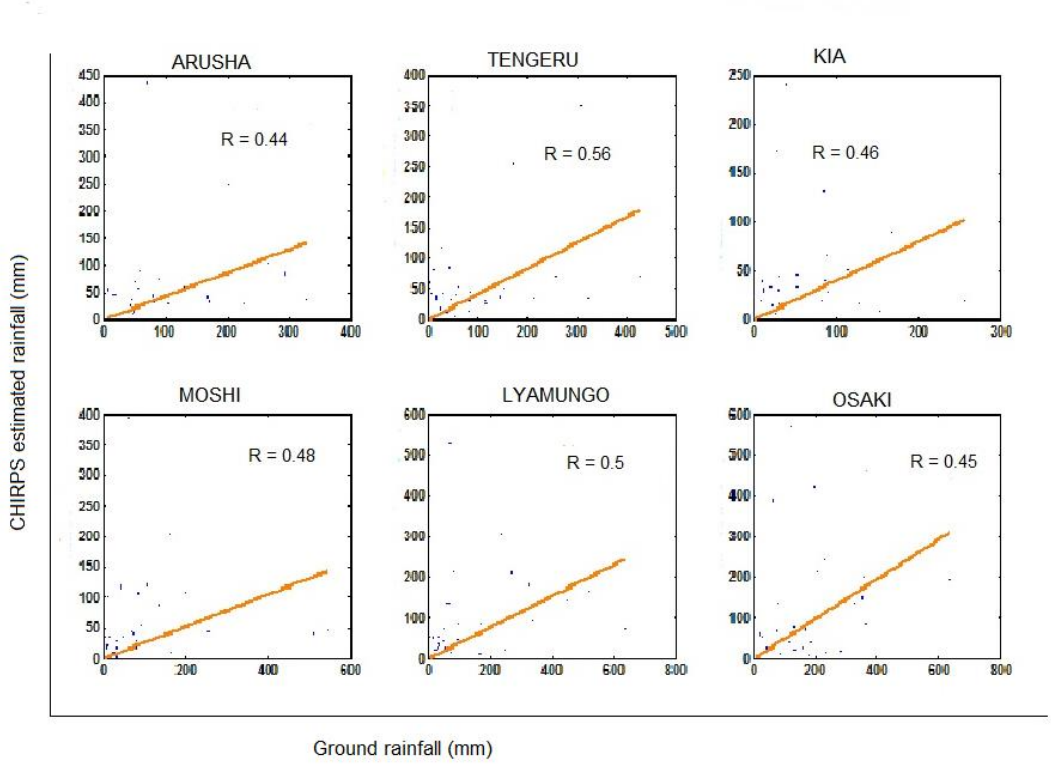

Figure 5.7: Monthly correlation between CHIRPS estimated rainfall and ground rainfall

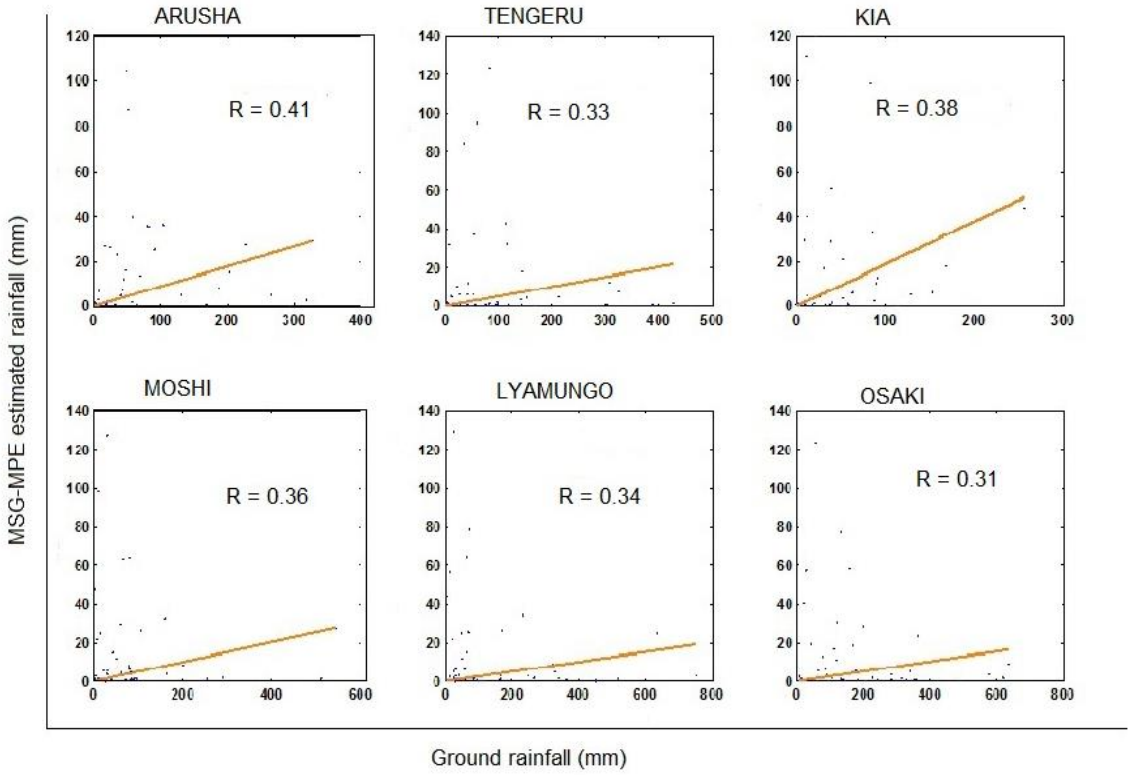

Figure 5.9: Monthly correlation between MSG-MPE estimated rainfall and ground rainfall

Bias Analysis

Different sources of biases calculated based on (section 4.2.5) are shown in Table 5.2 below. According to the analysis, it can be explained that the rainfall underestimation for both products is attributed to missed and false rainfall events. The missed rainfall events may be due to fewer sampling interval for TRMM which is limited to two overpasses per day and inability to catch short lived convective storms (Huffman et al., 2007b). The inability of MSG-MPE to record rainfall is due to its algorithm which is limited to convective rainfall. It assumes that colder clouds are more likely to produce more rain than warmer clouds (Heinemann & Kerényi, 2003). Also, orographic effects has not been considered in the algorithm, which causes MPE products to underestimate rainfall in mountainous areas (Heinemann & Kerényi, 2003). Thus, the poor performance of MSG-MPE in the study area is caused by orographic rainfall mostly due to orographic uplifting of moist air with warm clouds, which cannot be detected by the satellite with these algorithms. Moreover, the poor performance of CHIRPS satellite is due to its algorithm which was created to records cold clouds (Funk et al., 2014).

Table 5.2: Analysis of the decomposed bias

STATION	TRMM			MSG-MPE			CHIRPS		
	HIT	MISSED	FALSE	HIT	MISSED	FALSE	HIT	MISSED	FALSE
Arusha	140	287	241	59	37	78	68	361	82
Tengeru	100	398	164	61	26	80	57	444	86
KIA	72	212	167	33	21	91	40	246	101
Moshi	107	278	188	37	32	88	46	341	111
Lyamungo	324	343	485	56	47	64	67	603	90
Osaki	522	89	970	38	55	78	48	566	106

Detection Capability

The ability of, TRMM MSG-MPE and CHIRPS in rainfall detection has been evaluated by three categorical statistics (Table 5.3), namely Frequency Bias Index (FBI), Probability of Detection (POD) and False alarm Ratio (FAR). The POD and FBI values for TRMM ranges from 0.2 to 0.9, 0.5 to 2 respectively. TRMM underestimates rainfall events in four stations with FBI<1 and overestimate in two stations. Its FAR values range from 0.6 to 0.7 indicating the large fraction of non-events counts. POD values for MSG-MPE are higher in four stations while the lowest being 0.4 in Osaki station. Its FBI values which are greater than 1 indicate that there is an overestimation of rainfall in both stations, which might be due to false rainfall counts which is evident by large FAR. Also, CHIRPS satellite did not perform well in any of the three statistics. It has poor POD in all stations, an underestimation of rainfall and large number of non-events counts.

Table 5.3: Analysis of satellite detection capability

STATION	TRMM			MSG-MPE			CHIRPS		
	POD	FBI	FAR	POD	FBI	FAR	POD	FBI	FAR
Arusha	0.3	0.9	0.6	0.6	1.4	0.6	0.2	0.3	0.5
Tengeru	0.2	0.5	0.6	0.7	1.6	0.6	0.1	0.3	0.6
KIA	0.3	0.8	0.7	0.6	2	0.7	0.1	0.5	0.7
Moshi	0.3	0.8	0.6	0.5	1.8	0.7	0.1	0.4	0.7
Lyamungo	0.5	1.2	0.6	0.5	1.1	0.5	0.1	0.2	0.6
Osaki	0.9	2	0.7	0.4	1.2	0.7	0.1	0.3	0.7

5.3.2. Areal Comparison

This section compares satellite and ground rainfall at sub-catchments scale. An interpolated ground rainfall by using the Thiessen polygon method was compared with an average rainfall of pixels within that sub-catchment. As it was done in point to pixel comparison, the performance of satellite rainfall estimates was assessed by statistical and categorical analysis (sections 4.2.4 – 5). As it was the case in point to pixel comparison, daily comparison showed a weak correlation with ground rainfall. The RMSE for MSG-MPE and CHIRPS were ranging from 8 – 15 mm day^{-1}, while the negative mean differences (-6 to -2 mm) indicate that both satellites underestimated areal ground rainfall. The areal TRMM rainfall estimation has lower RMSE ranging from 6 – 9 mm day^{-1} and the correlation coefficient between 0.1 and 0.2. However, monthly comparison of the areal TRMM estimated rainfall has the correlation coefficient above 0.5 (Figure 5.10) indicating a better fit of the TRMM to ground rainfall in a monthly basis. The areal MSG-MPE and CHIRPS satellite rainfall estimate have the correlation coefficient ranging between 0.3 and 0.5 showing an improvement as compared to daily analysis.

The decomposed bias Table 5.4 shows that the missed and false bias contributed significantly to the total bias in all Satellite Rainfall Estimates (SRE) products. However, TRMM has the highest number of hit rainfall events as compared to CHIRPS and MSG-MPE satellites. The POD of TRMM ranges from 0.2 to 0.7 while for MSG-MPE it range from 0.5-0.6 (Table 5.5). TRMM performed better in terms of POD in sub-catchment two, whereas MSG-MPE performs fairly well in all sub-catchments. CHIRPS satellite has POD range from 0.1 to 0.2, which proves its inability of detecting rainfall in Kikuletwa catchment.

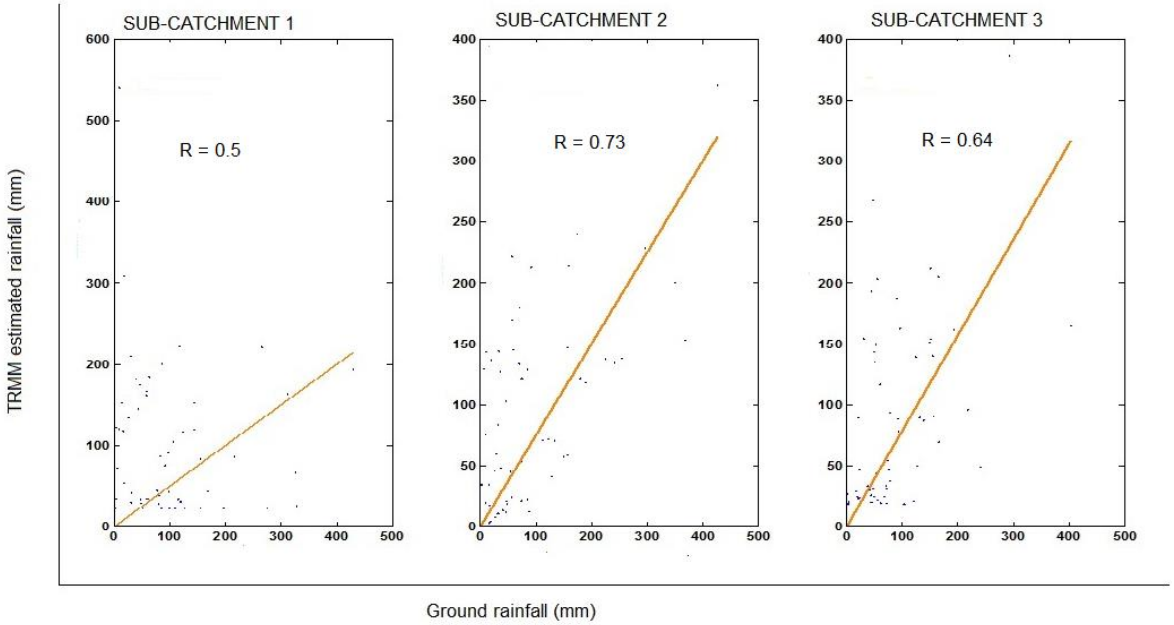

Figure 5.10: Monthly correlation between TRMM estimated rainfall and ground rainfall in Sub-catchments

Table 5.4: Analysis of the decomposed bias based on sub-catchments

SUBCATCHMENTS	TRMM			MSG-MPE			CHIRPS		
	HIT	MISSED	FALSE	HIT	MISSED	FALSE	HIT	MISSED	FALSE
SUBCATCHMENT 1	100	398	164	80	60	95	68	560	350
SUBCATCHMENT 2	606	233	617	60	67	80	80	700	280
SUBCATCHMENT 3	328	546	239	100	90	150	132	580	300

Table 5.5: Analysis of satellite detection capability based on sub-catchments

SUBCATCHMENTS	TRMM			MSG-MPE			CHIRPS		
	POD	FBI	FAR	POD	FBI	FAR	POD	FBI	FAR
SUBCATCHMENT 1	0.2	0.5	0.6	0.6	1.3	0.5	0.1	0.7	0.8
SUBCATCHMENT 2	0.7	1.5	0.5	0.5	1.1	0.6	0.1	0.5	0.8
SUBCATCHMENT 3	0.4	0.6	0.4	0.5	1.3	0.6	0.2	0.6	0.7

5.4. Bias correction for TRMM rainfall data

Comparison of SRE products with ground rainfall indicated that the TRMM is the most accurate in rainfall detection in the temporal scale among the three products (Tables 5.4 and section 5.3.2). It is for that reason TRMM has been chosen for further processing and will be used in modelling. Although there are differences between TRMM estimation and ground rainfall, those differences can be minimized by a correction factor. Equation 4.12 was used to correct TRMM data in each sub catchment. Then, the CDF-matching method was applied to correct satellite rainfall distribution in the study area. The concept behind this method is to match the CDF's of the corrected TRMM and ground rainfall in order to reduce the biases in the estimated satellite rainfall. Figure 5.11 presents the CDF's of the ground rainfall, TRMM and the corrected TRMM rain values showing the better fit of the corrected TRMM and ground CDF's.

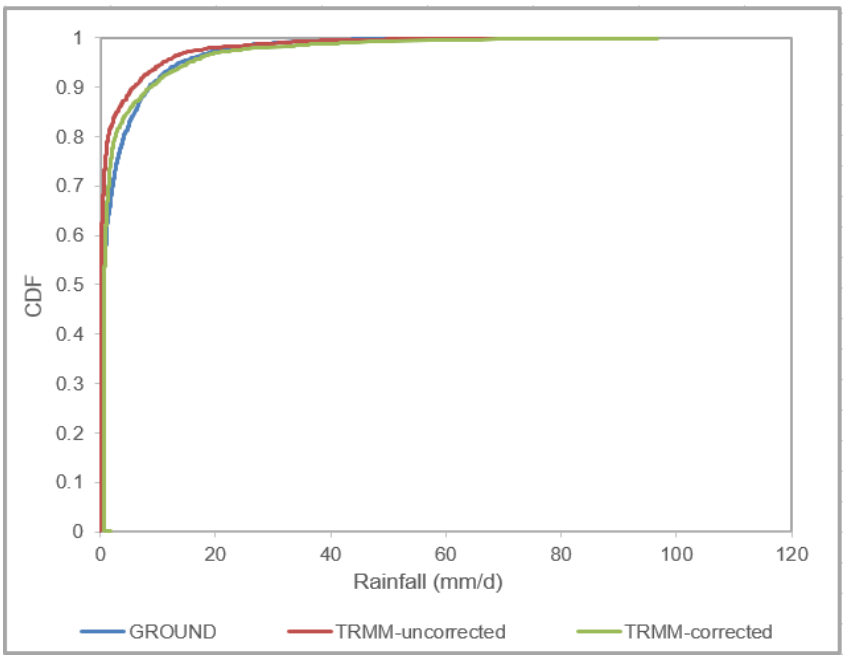

Figure 5.11: Cumulative Distribution Function (CDF) for ground, uncorrected TRMM and corrected TRMM rainfall

The relationship between ground and TRMM rainfall has improved after bias correction with a lower RMSE ranging from 5 to 8 mm day^{-1}, Mean Difference ranging from -0.04 to 0.08 and a correlation coefficient of 0.4.

5.5. Spatial rainfall distribution

Spatial rainfall variability analysis within the catchment (Figure 5.12) demonstrate the occurrence of higher amount of rainfall in the northern side along the mountain's slopes and lower rainfall is observed in the south and western side for ground observations. The TRMM and CHIRPS have a spatial pattern similar to that of ground observation for higher rainfall, but has low rainfall in large part of the catchment. In contrary, MSG-MPE shows lower rainfall in the northern part and more rainfall in the southern and western part. This can be explained by its algorithm which is suitable for convective rainfall rather than orographic rainfall (Heinemann & Kerényi, 2003).

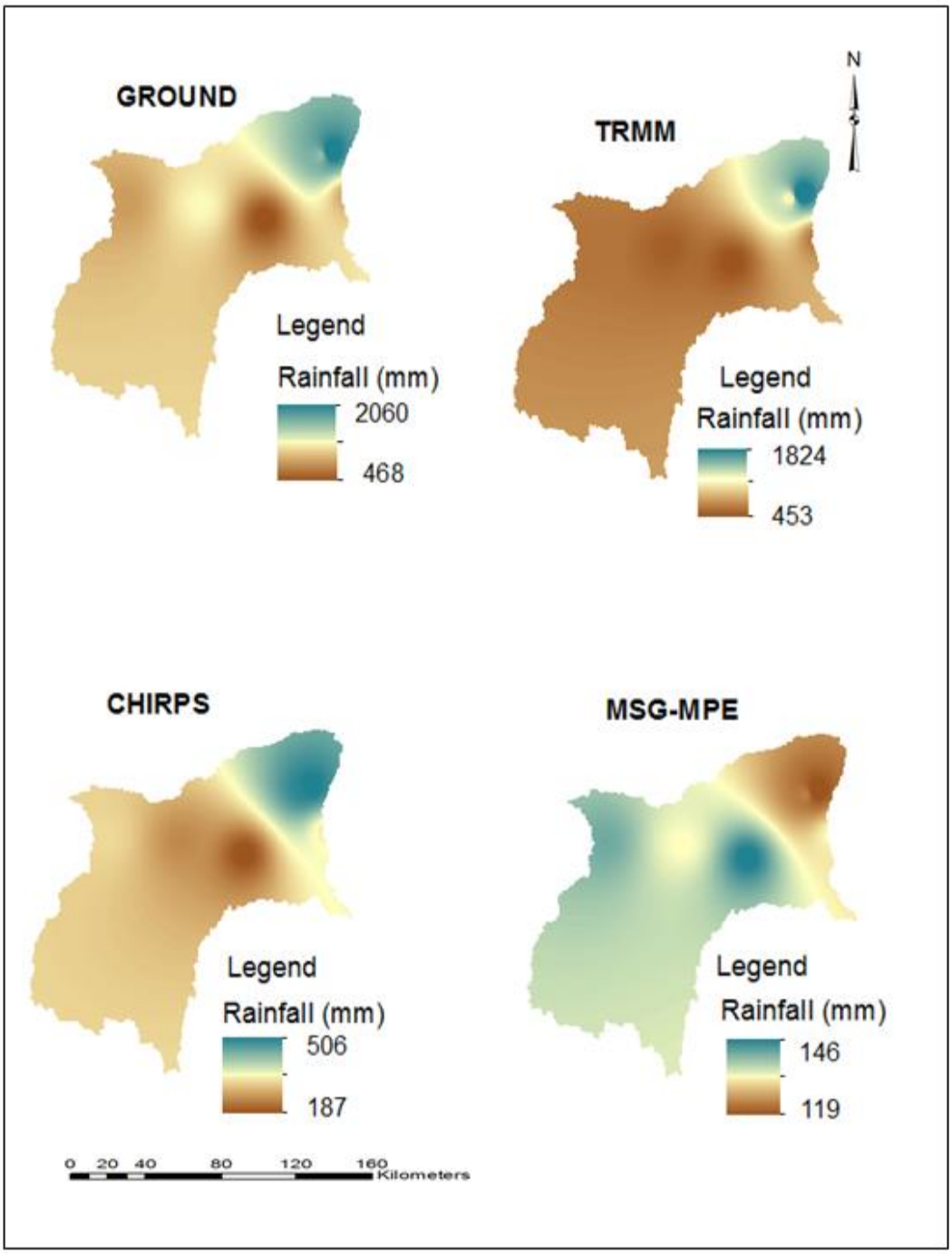

Figure 5.12: Spatial distribution of mean annual rainfall for Ground, TRMM, CHIRPS and MSG-MPE.

5.6. Model Calibration and Sensitivity Analysis Results

HBV-light Model Calibration

The model was manually calibrated for the period of 2011 to 2013 until an optimum parameter set (Table 5.6) that represents the catchment was attained. Prior model parameters ranges (Table 5.6) were taken from (J. Seibert & Vis, 2012) and all the optimized parameters fall within that range. Further, two objective functions as discussed in section 4.3.2 were used to assess the performance of the model in simulating catchments stream flow. Figure 5.13 and Table 5.7 shows the results of the model calibration for the four different data sets (ground, merged, uncorrected and corrected TRMM rainfall).

Table 5.6: Prior model parameter range and Optimized model parameters

Model Parameter	Prior Model Parameter Range		Optimized Model Parameters			
			Ground Data	TRMM Uncorrected	TRMM Corrected	Merged Data
	Minimum	Maximum				
FC (mm)	125	800	550	480	450	500
LP	0.1	1	0.1	0.1	0.1	0.1
BETA	1	6	2	1.5	2	2
ALPHA	0.1	3	1	1.2	1	1.5
K1 (d^{-1})	0.0005	0.15	0.09	0.15	0.15	0.15
K2 (d^{-1})	0.0005	0.15	0.006	0.001	0.002	0.006
MAXB (d)	0	100	2.1	1	1	2
PART	0	1	0.08	0.2	0.07	0.08
DELAY(Δt)	0	∞	1	1	1	1

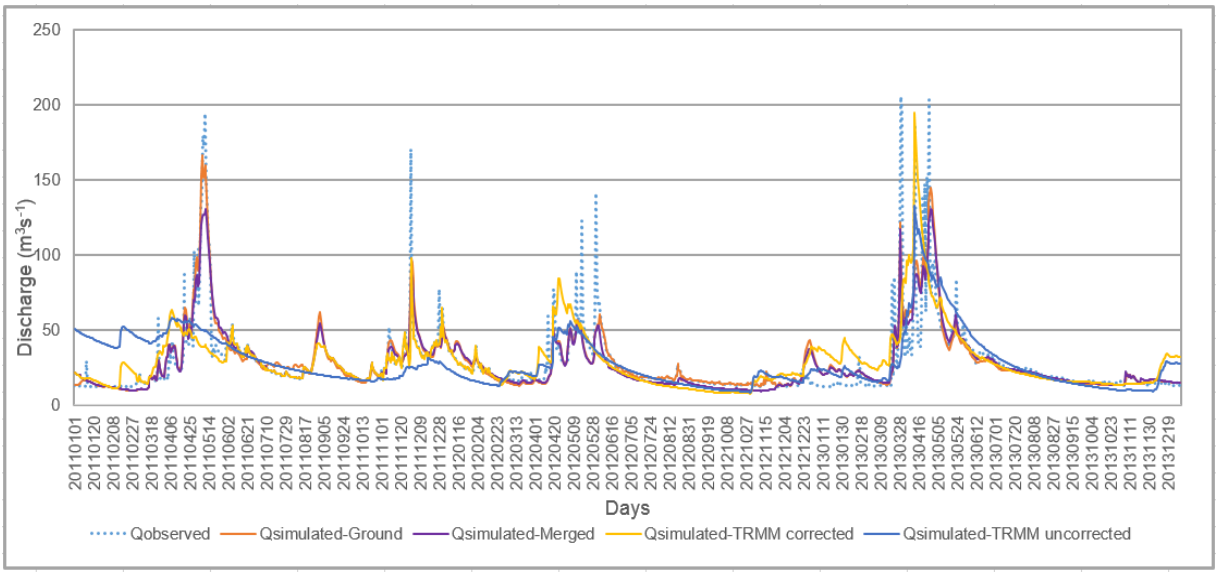

Figure 5.13: Observed and simulated discharge during calibration period

Stream flow simulation using ground rainfall has the better results as compared to the other simulations. It has NS value of 0.8 and RVE of 1.4 % which is considered as a reasonable performance because its NS value ranges between 0.6 to 0.8 and RVE between -5% to 5% (M. Rientjes, 2014). Also, when looking at the simulated hydrographs it is seen that the model was able to depict the shape and trend of the observed flow, and the base-flow was well simulated except in March, 2011 and March - April, 2012 where there is an underestimation. Slight overestimation of the base-flow is noticed in July-August, 2011 and in January, 2013. The peaks were well simulated in May, 2011 and fairly in December, 2011 while the rest of simulation period was underestimated. It is also seen from the simulated discharge that there is a delay of time to peak in some of the events. The underestimation/overestimation of the base-flow/peaks can be attributed to observation errors during measurements or from several lumped parameters contributing to the model uncertainty. Another reason could be due to rainfall interpolation errors which might not capture the areal variability of rainfall pattern. This is because the rainfall network is only located in the northern side of the catchment while none exist in the southern part. Also, there are springs and swampy areas in the catchment which could not be well represented in the model.

Table 5.7: Model calibration results

Objective Function	Ground Data	TRMM Uncorrected	TRMM Corrected	Merged Data
NS	0.8	0.3	0.5	0.6
RVE (%)	1.4	4.3	5	2

Stream flow simulated by using uncorrected TRMM has NS value of 0.3 which indicating a poor performing model. However, modelling results have improved to NS value of 0.5 when the bias corrected TRMM values have been used. Their RVE are 4.3 % and 5% for uncorrected and corrected TRMM values respectively. The model was able to reproduce the distribution of base-flow in both (TRMM corrected and uncorrected rainfall) despite an overestimation which is seen in the uncorrected TRMM data from January – June, 2011 and in December, 2012 – March, 2013 for both TRMM products. Also there is an underestimation of the base-flow in October - March, 2012 and in November, 2012 to March, 2013 for TRMM uncorrected. Moreover, the peaks were poorly represented in both data sets except in April, 2013 for the corrected TRMM rainfall in which, also a delay in time to peak is noticed. The poor performance of the model when using satellite data can be due to little rainfall which is caused by the failure of the satellites to detect rainfall or the shorter calibration time (Su et al., 2008).

Stream flow simulation based on the merged rainfall (ground and TRMM) data yielded good NS value of 0.6, which is considered as reasonable performance. Like in the other simulations, the shape of the base-flow was well captured, but slight underestimation is seen in July – August, 2011 and June – November, 2012. Base-flow overestimation is noticed in January, 2013. In addition, the peaks were underestimated throughout the simulation period.

Model Sensitivity Analysis

Model sensitivity analysis was performed in order to evaluate the response of the model when changing the input parameters. In this study, the sensitivity analysis was performed by changing one parameter at a time. This was done by decreasing and increasing the model parameter values from -100% to 100% by 20% interval. The sensitive parameters were first determined when fitting the base-flow and later when fitting the peaks. Two parameters (K2 and FC) were found sensitive when fitting the base-flow and three parameters (ALPHA, K1 and PART) when fitting the peaks (Figure 5.14).

It is clearly noticed from the plot that decreasing K2 values causes a decrease in model efficiency while the efficiency remains nearly the same on the value increase. This is because K2 is a recession coefficient, which determines flow in the lower zone storage and causes a large amount of base-flow to be generated when low values are assigned to the model. But when higher values are assigned to the model, the amount of base-flow is reduced as more water will leave the system. Moreover, field capacity (FC) parameter which represents the maximum soil moisture storage causes the model efficiency to decrease when its value was decreased, while the NS remain almost the same on the value increase. A decrease in FC parameter value lowers the amount of water stored in the soil and generate a lot of runoff, which affects the volume of water in the simulated hydrograph. Also, if there is a low amount of water in the soil it means even recharge to the ground water will be low and cause base-flow to decrease. Similarly, when FC values are increased there will be more recharge and base-flow will increase while the amount of runoff will decrease.

When looking on the PART parameter, it is seen that the model response greatly in both the increase and decrease in its value. This is because, PART parameter controls the amount of water coming from the soil zone to the upper zone, leading to runoff. If you assign a large PART value it means a lot of water (runoff) will be generated from the upper zone which makes a large error in volume and hence poor NS. Also when PART value was set to low values/zero, there were no peak flows rather than the base-flow. K1 parameter determines the magnitude and recession of the peaks. An increase of K1 values causes an increase in discharge in the upper zone which resulted in the high peaks. While decreasing K1 values lead to low runoff and the peaks were low as well. The parameter Alpha is a measure of the non-linearity and controls the shape of the hydrograph. Decrease of its values leads to an abrupt lowering of the model efficiency than when its values are increased. A decrease of Alfa value resulted in constant discharge (no peaks) while an increase of its value causes the simulated hydrograph to have very high peak.

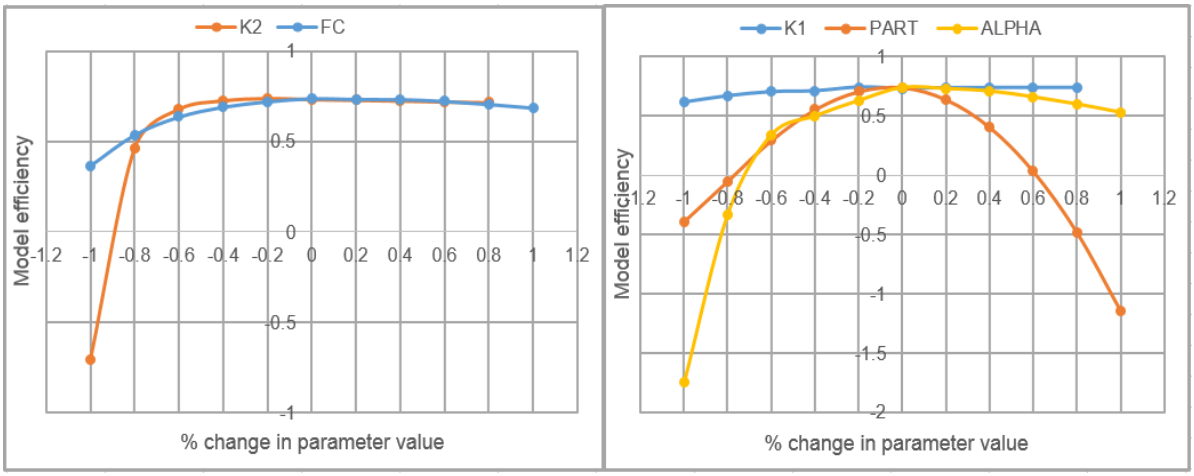

Figure 5.14: Sensitivity analysis results (Left: Base-flow; Right: Peaks)

5.6.1. Comparison of Water Balance Components

Water balance components (actual evapotranspiration and simulated discharge) were assessed for all the input data sets applied to the model. It has been observed that different rainfall data sources resulted in different water balance components. Furthermore, the results show that the larger portion of rainfall falling in the catchment is stored (evident by larger field capacity values during calibration) and released afterwards by base-flow and evapotranspiration. This phenomenon can be explained by low discharge values and higher actual ET in the water balance assessment (Table 5.8).

Table 5.8: Assessment of the water balance components

Water Balance Components (mm y^{-1})	Ground Data	TRMM Uncorrected	TRMM Corrected	Merged Data
Rainfall	1324	918	1199	1297
Actual ET	1155	900	1130	1143
Q-simulated	140	144	142	141
Closure Term	29	-126	-73	13

Closure term in the water balance component assessment (P – ET - Q) is not equal to zero because, HBV-Light model considers changes in water storage within the catchment (SMHI, 2008). Changes in water storage can be from changing in soil moisture contents, upper and lower storage zones, and from the lakes. The simulated catchment is not an isolated catchment, it receives water from the two interconnected upstream catchments and there are also springs and swampy within the catchment. In addition, the areas with springs and swampy have been assigned to the model in which interactions between ground and surface water occurs. All these contributed to an addition amount of water to the catchment which leads to the balance closure term not to be zero. Another reason might be due uncertainty of an estimated PET from MOD 16. An estimated PET seems to be higher (2200 mm yr^{-1}) as compared to the range found in literature 1800 to 2000 mm yr^{-1} (IUCN, 2009). The larger PET values can cause an increase of actual ET values if there is much water in the soil. Also, the changes of actual ET in rainfall amount is attributed to changes in soil moisture storage which were different during model calibration.

There are several hydrological studies which have been done by using the HBV model and resulted in a water balance closure term of not equal to zero. For example, Setegn et al., (2011) conducted a study of hydrological balance of Lake Tana, Ethiopia and resulted in a water balance closure term of 85 mm. All these results show that the model considers changes in water storage in a catchment.

5.7. Model Validation

Model validation was performed with an independent set of parameters for the year 2014. This was done in order to assess the reliability of the model because calibrated models are associated with uncertainties from input parameters or the selected model structure. So, the model has to be tested for its validity prior to use. If the model will accurately simulate the stream flow in this period, it is assumed that it will be able to simulate well in other periods (M. Rientjes, 2014).

Generally, the model was able to capture the distribution of base-flow with the ground and the merged rainfall data, but overestimated by TRMM data sets (Table 5.9 and Figure 5.15). An overestimation of the base-flow can be attributed to too much rainfall recorded by the TRMM satellite in the year 2014. Moreover, the peaks were fairly represented by the ground rainfall but not represented in the other simulations. The poor model performance during this period can be due to shorter simulation period or poor quality of the observed data (rainfall and discharge). As it can be observed from the plot that there is a significant amount of rainfall in May, which is not well represented in the discharge data. Another reason could be that the HBV model fails to represents the complex system of the catchment, as there is a lot of abstraction in dry season and very little in rainy season.

Table 5.9: Validation results

Objective Function	Ground Data	TRMM Uncorrected	TRMM Corrected	Merged Data
NS	0.2	0.02	0.01	0.1
RVE (%)	5	10	13	9

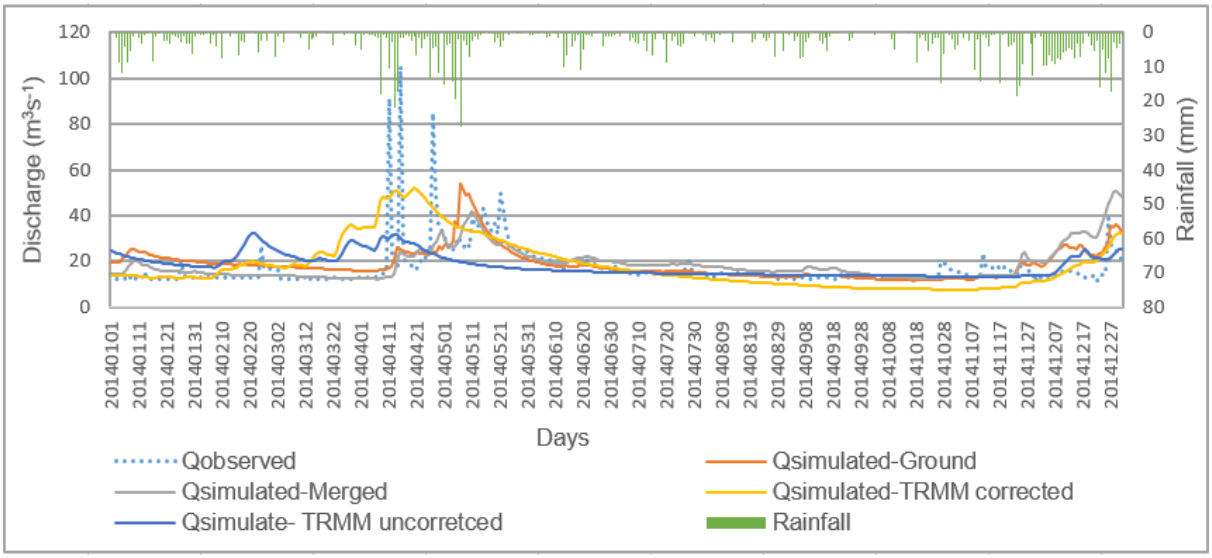

Figure 5.15: Observed and simulated discharge during validation period

6. CONCLUSION AND RECOMMENDATION

6.1. Conclusion

The objective of this study was to assess if satellite rainfall data can be used to improve the assessment of stream flow in the Kikuletwa catchment. Satellite products which were used are TRMM, CHIRPS and MSG-MPE; and the assessment was done for five years from 2010-2014. Initially, the comparison of satellite and ground rainfall data was performed to see the relation between them. Statistical methods were used to assess the fit of satellite rainfall in representing catchment's rainfall. Both satellite data showed bias when compared to the ground rainfall. However, TRMM was selected for further processing as it has temporal scale similar to the ground rainfall and it was later adjusted before modelling. The Cumulative Distribution Function (CDF)-matching method was used to correct TRMM rainfall distribution in the study area. The merging technique was also applied between satellite and TRMM data. Afterwards, HBV-Light hydrological model was used to simulate the stream flow discharge by using ground, merged, corrected and uncorrected TRMM rainfall data. The model was calibrated for three years from 2011-2013, validated for one year 2014 and time series of 2010 was used in warming up the model. Sensitivity analysis was also performed to see the response of the model prior to parameter change.

Comparison of satellite and ground rainfall was done in two ways, point to pixel and areal comparison (based on sub-catchments) in daily and monthly temporal scales. Comparison results on a daily scale indicating the inability of all products to capture rainfall in the study area. The rainfall underestimation (evident by negative mean differences) is observed in both products. However, monthly comparison has resulted in good correlation coefficient of above 0.5 for the TRMM and between 0.3 and 0.5 for CHIRPS and MSG-MPE. Bias corrected TRMM has RMSE ranging from 5 to 8 mm day^{-1} and R of 0.3. Satellite rainfall detection capabilities was assessed and MSG was found to have POD values ranging from 0.4 to 0.7 in most events while TRMM shows good POD value of 0.9, 0.7 and 0.5 for three events and other events have POD values < 0.4. CHIRPS products have the worst POD values ranging from 0.1 to 0.2 in all the events. However, missed and false bias were the main components which contributed to the differences between measured and satellite rainfall during the study period. The good POD values for MSG-MPE can be attributed to its higher spatial resolution. Further, the failure of satellite products to capture rainfall can be due to lower sampling interval and its tendency to underestimate heavy rainfall for TRMM (Dinku et al., 2007) and as reported by Heinemann & Kerényi, (2003) for MSG-MPE and Funk et al., (2014) for CHIRPS can be attributed to their algorithm which were configured for and most suitable for convective rainfall and in which orographic effects has not been considered.

Spatial rainfall distribution analysis with ground rainfall shows the occurrence of higher rainfall in the northern side of the catchment and little in the other parts. TRMM and CHIRPS satellites were able to depict that pattern, but MSG-MPE spatial pattern shows much rainfall in the low lands and very little along the slopes of the mountain.

When the rainfall from the ground, TRMM, MSG-MPE and CHIRPS were compared to the amount of discharge produced in the catchment, ground rainfall showed good correlation with discharge. Even the catchment responded well to the heavy rainfall events by producing a high amount of discharge. TRMM rainfall estimates agrees with the ground based rainfall for about 64% of the annual rainfall that occurs in the heavy rain season. It also has a temporal pattern similar to the ground rainfall as it was able to depict the bimodal rainfall pattern within the catchment. Hence, TRMM is considered suitable for hydrological modelling. Rainfall estimates from CHIRPS and MSG-MPE were too low for hydrological modelling.

CHIRPS was able to capture only 35% while MSG-MPE was able to capture only 6% of rainfall during rainy season. The failure of these two satellites to represent amount of rainfall is due to the large number of missing values for MSG-MPE and no rain values (zeros) for CHIRPS.

The model was calibrated by trial and error method for the period of 2011 to 2013. The modelling calibration results by using ground rainfall data shows the best performance with Nash-Sutcliffe coefficient of efficiency (NS) value of 0.8 and Relative Volumetric Error (RVE) of 1.4 % while NS value for the merged data is 0.6 and RVE of 2 % which also indicating a good performance. The results for corrected and uncorrected TRMM are NS 0.5, 0.3 with RVE of 5 % and 4.3 % respectively which indicates that the model did not perform well on those data. Moreover, the model was able to capture the distribution of base-flow but the peaks were not well represented for both data sets. Validation results were not satisfactory for both data sets. The NS and RVE values for ground and merged data are 0.2, 0.1 and 5% and 9% respectively in which the base-flow was fairly represented but the peaks were not captured. TRMM data sets (uncorrected and corrected) have NS values of 0.02, 0.01 and RVE of 10% and 13% respectively. The base-flow was overestimated, which causes a large difference in the volume between ground and estimated satellite rainfall.

Sensitivity of the model was assessed based on the calibration parameters while first fitting the base-flow followed by the peaks. Parameters K2 and FC were found sensitive when fitting the base-flow while K1, PART and ALPHA while fitting the peaks.

The water balance components were also assessed and it was observed that the system stores much water, which is released afterwards by base-flow and evapotranspiration. This phenomenon can be explained by low discharge values and higher actual ET which were observed in the water balance assessment. It has also been observed that different rainfall data sources resulted in different water balance components. Higher actual ET was calculated from ground rainfall data and the value has decreased in other data sets. However, little discharge has been generated from rainfall in ground observations and more discharge from other data sets (TRMM corrected and uncorrected and merged rainfall data).

Comparison of satellite and ground rainfall data sets show that the satellites were not able to represent rainfall in Kikuletwa catchment in a daily bases, but a good correlation was attained in a monthly scale. However, TRMM is good in terms of temporal resolution and was able to capture about 64% of catchment rainfall during higher rainfall season and thus, it is a good product for hydrological modelling. But, its spatial resolution (27km) is not representative of the rainfall distribution in the catchment. MSG-MPE has good spatial coverage (3km) which can capture well the spatial variability of rainfall, but cannot be used for modelling purposes because of larger missing values (more than 80%) during the study period. CHIRPS satellite data have no missing values, but a lot of zeros (about 90%) and a lot of missed rainfall counts which is considered not suitable for hydrological modelling. Since merging of ground rainfall and TRMM estimated rainfall produced a model with good NS value (0.6), a merging technique can be considered as the way of improving satellite estimations as it takes the advantages of both data set and produce more reliable data sources which can be used in hydrological modelling.

6.2. Recommendations

Rainfall gauge stations are unevenly distributed within the catchment which makes the calculations of rainfall difficult. Most of the stations are located in the northern side with none in the southern side. This also resulted in errors when computing catchment areal rainfall. This calls for special attention (for responsible authorities) of considering installing rainfall station in order to have even distribution of stations for easier monitoring and also for good and consistency data which might be used in hydrological and environmental studies.

Since monthly comparison of ground and satellite rainfall data has shown good results in this study and in some of the studies by Worqlul et al., (2014) and Meng et al., (2014a), it is recommended that a monthly comparison to be considered for analysis with larger number of ground rainfall stations and longer simulation period.

TRMM shows better agreements with ground in temporal scale, so a downscaling method is also recommended for the TRMM data in order to get a good spatial resolution data which can better represent the spatial variation of rainfall within the catchment.

The HBV-Light model calibration resulted in a good model performance in Kikuletwa catchment when ground and merged rainfall data were used. However, the model performance could increase if longer calibration time was used. It is advices that longer calibration time to be considered for the coming studies.

LIST OF REFERENCES

Ababa, A. (2011). RAINFALL-RUNOFF MODELS ON MUGER Department of Civil Engineering Addis Ababa Institute of, (January).

Abiola, S. F., Mohd-mokhtar, R., Ismail, W., Mohamad, N., & Mandeep, J. S. (2013). Categorical statistical approach to satellite retrieved rainfall data analysis in Nigeria, *8*(43), 2123–2137. doi:10.5897/SRE2013.5512

Arnold, J. G., Muttiah, R. S., Srinivasan, R., & M, A. P. (2000). Regional estimation of base flow and groundwater recharge in the upper mississippi river basin.

Behrangi, A., Lebsock, M., Wong, S., & Lambrigtsen, B. (2012). On the quantification of oceanic rainfall using spaceborne sensors. *Journal of Geophysical Research: Atmospheres*, *117*(D20), n/a–n/a. doi:10.1029/2012JD017979

Beighley, R. E., Ray, R. L., He, Y., Lee, H., Schaller, L., Andreadis, K. M., … Shum, C. K. (2011). Comparing satellite derived precipitation datasets using the Hillslope River Routing (HRR) model in the Congo River Basin. *Hydrological Processes*, *25*(20), 3216–3229. doi:10.1002/hyp.8045

Bhavani, R. (2013). COMPARISION OF MEAN AND WEIGHTED ANNUAL RAINFALL IN ANANTAPURAM DISTRICT, *2*(7).

Dinku, T., Ceccato, P., Grover- Kopec, E., Lemma, M., Connor, S. J., & Ropelewski, C. F. (2007). Validation of satellite rainfall products over East Africa's complex topography. *International Journal of Remote Sensing*, *28*(May 2015), 1503–1526. doi:10.1080/01431160600954688

Feng, P., & Li, J. Z. (2008). Scale effects on runoff generation in meso-scale and large-scale sub-basins in the Luanhe River Basin. *Hydrology and Earth System Sciences Discussions*, *5*(April), 1511–1531. doi:10.5194/hessd-5-1511-2008

Funk, C. C., Peterson, P. J., Landsfeld, M. F., Pedreros, D. H., Verdin, J. P., Rowland, J. D., … Verdin, a. P. (2014). A quasi-global precipitation time series for drought monitoring. *U.S. Geological Survey Data Series*, *832*, 4. doi:http://dx.doi.org/110.3133/ds832

Habib, E., Larson, B. F., & Graschel, J. (2009). Validation of NEXRAD multisensor precipitation estimates using an experimental dense rain gauge network in south Louisiana. *Journal of Hydrology*, *373*, 463–478. doi:10.1016/j.jhydrol.2009.05.010

Haile, A. T., Habib, E., & Rientjes, T. (2013). Evaluation of the climate prediction center (CPC) morphing technique (CMORPH) rainfall product on hourly time scales over the source of the Blue Nile River. *Hydrological Processes*, *27*(12), 1829–1839. doi:10.1002/hyp.9330

Haque, R. M. F., Maskey, S., Uhlenbrook, S., & Mul, M. (2013). Technical Paper Validation of TRMM Rainfall for Pangani River Basin in Tanzania 1, *1*(1), 30–40.

Heinemann, T., & Kerényi, J. (2003). The EUMETSAT Multi Sensor Precipitation Estimate (MPE): Concept and validation. … *from EUMETSAT Website: Http://www. Eumetsat* …. Retrieved from http://www.isac.cnr.it/~ipwg/meetings/monterey-2004/pres/Heinemann/mpef/pdf/EUMETSAT_UC2003_MPE.pdf

Huffman, G. J., Bolvin, D. T., Nelkin, E. J., Wolff, D. B., Adler, R. F., Gu, G., … Stocker, E. F. (2007a). The TRMM Multisatellite Precipitation Analysis (TMPA): Quasi-Global, Multiyear, Combined-

Sensor Precipitation Estimates at Fine Scales. *Journal of Hydrometeorology*, *8*(1), 38–55. doi:10.1175/JHM560.1

Huffman, G. J., Bolvin, D. T., Nelkin, E. J., Wolff, D. B., Adler, R. F., Gu, G., … Stocker, E. F. (2007b). The TRMM Multisatellite Precipitation Analysis (TMPA): Quasi-Global, Multiyear, Combined-Sensor Precipitation Estimates at Fine Scales. *Journal of Hydrometeorology*, *8*, 38–55. doi:10.1175/JHM560.1

IUCN. (2009). Pangani Basin : Pangani Basin :

Jeniffer, K., Su, Z., Woldai, T., & Maathuis, B. (2010). Estimation of spatial–temporal rainfall distribution using remote sensing techniques: A case study of Makanya catchment, Tanzania. *International Journal of Applied Earth Observation and Geoinformation*, *12*, S90–S99. doi:10.1016/j.jag.2009.10.003

Joyce, R. J., Janowiak, J. E., Arkin, P. a., & Xie, P. (2004). CMORPH: A Method that Produces Global Precipitation Estimates from Passive Microwave and Infrared Data at High Spatial and Temporal Resolution. *Journal of Hydrometeorology*, *5*, 487–503. doi:10.1175/1525-7541(2004)005<0487:CAMTPG>2.0.CO;2

Katimon, A., Khairi, A., & Wahab, a B. D. (2007). Hydrologic Characteristics of a Drained Tropical. *Water*, *38*, 39–53.

Kidd, C., & Levizzani, V. (2010). Status of satellite precipitation retrievals. *Hydrology and Earth System Sciences*, *15*, 1109–1116. doi:10.5194/hess-15-1109-2011

Li, X., Zhang, Q., & Xu, C.-Y. (2013). Assessing the performance of satellite-based precipitation products and its dependence on topography over Poyang Lake basin. *Theoretical and Applied Climatology*, *115*(3-4), 713–729. doi:10.1007/s00704-013-0917-x

Linus, K. M., & Pudensiana, C. S. (2014). Climate change and decline in water resources in Kikuletwa Catchment, Pangani, Northern Tanzania. *African Journal of Environmental Science and Technology*, *8*(1), 58–65. doi:10.5897/AJEST2013.1597

Maathuis, B. H. P., & Wang, L. (2006). Digital Elevation Model Based Hydro-processing. *Geocarto International*, *21*, 21–26. doi:10.1080/10106040608542370

Maathuis, B., & Mannaerts, C. (2013). In Situ and Online Data Toolbox, (July).

Mashingia, F., Mtalo, F., & Bruen, M. (2014). Validation of remotely sensed rainfall over major climatic regions in Northeast Tanzania. *Physics and Chemistry of the Earth, Parts A/B/C*, *67-69*, 55–63. doi:10.1016/j.pce.2013.09.013

Meng, J., Li, L., Hao, Z., Wang, J., & Shao, Q. (2014a). Suitability of TRMM satellite rainfall in driving a distributed hydrological model in the source region of Yellow River. *Journal of Hydrology*, *509*(November 1997), 320–332. doi:10.1016/j.jhydrol.2013.11.049

Meng, J., Li, L., Hao, Z., Wang, J., & Shao, Q. (2014b). Suitability of TRMM satellite rainfall in driving a distributed hydrological model in the source region of Yellow River. *Journal of Hydrology*, *509*(November 1997), 320–332. doi:10.1016/j.jhydrol.2013.11.049

Mu, Q., Zhao, M., & Running, S. W. (2011). Improvements to a MODIS global terrestrial evapotranspiration algorithm. *Remote Sensing of Environment*, *115*(8), 1781–1800. doi:10.1016/j.rse.2011.02.019

Müller, M. F., & Thompson, S. E. (2013). Bias adjustment of satellite rainfall data through stochastic modeling: Methods development and application to Nepal. *Advances in Water Resources*, *60*, 121–134. doi:10.1016/j.advwatres.2013.08.004

Mutiga, J. K. (2011). *PLANNING OF SYSTEM INNOVATIONS IN WATERSHEDS : SPATIAL MAPPING OF ENVIRONMENTAL AND HYDROLOGICAL*.

Mwamila, T. B., Kimwaga, R. J., & Mtalo, F. W. (2008). Eco-hydrology of the Pangani River downstream of Nyumba ya Mungu reservoir, Tanzania. *Physics and Chemistry of the Earth, Parts A/B/C*, *33*(8-13), 695–700. doi:10.1016/j.pce.2008.06.054

Ndomba, P., Mtalo, F., & Killingtveit, A. (2008). SWAT model application in a data scarce tropical complex catchment in Tanzania. *Physics and Chemistry of the Earth, Parts A/B/C*, *33*(8-13), 626–632. doi:10.1016/j.pce.2008.06.013

Nebiyu Solomoni. (2013). Error in high-resolution satellite rainfall products in streamflow prediction in Birr Watershed, Ethiopia, (May).

Notter, B., Hurni, H., Wiesmann, U., & Ngana, J. O. (2013). Evaluating watershed service availability under future management and climate change scenarios in the Pangani Basin. *Physics and Chemistry of the Earth, Parts A/B/C*, *61-62*, 1–11. doi:10.1016/j.pce.2012.08.017

Ouyang, S., Puhlmann, H., Wang, S., von Wilpert, K., & Sun, O. (2014). Parameter uncertainty and identifiability of a conceptual semi-distributed model to simulate hydrological processes in a small headwater catchment in Northwest China. *Ecological Processes*, *3*, 14. doi:10.1186/s13717-014-0014-9

Piani, C., Weedon, G. P., Best, M., Gomes, S. M., Viterbo, P., Hagemann, S., & Haerter, J. O. (2010). Statistical bias correction of global simulated daily precipitation and temperature for the application of hydrological models. *Journal of Hydrology*, *395*(3-4), 199–215. doi:10.1016/j.jhydrol.2010.10.024

Rientjes, M. (2014). Modelling in Hydrology, (March).

Rientjes, T. H. M., Haile, a. T., Kebede, E., Mannaerts, C. M. M., Habib, E., & Steenhuis, T. S. (2011). Changes in land cover, rainfall and stream flow in Upper Gilgel Abbay catchment, Blue Nile basin - Ethiopia. *Hydrology and Earth System Sciences*, *15*(2008), 1979–1989. doi:10.5194/hess-15-1979-2011

Searcy, J. K., & Hardison, C. H. (1960). Double-Mass Curves. *WaterSupply Paper 1541B*, 66. doi:http://udspace.udel.edu/handle/19716/1592

Seibert, J. (2005). User ' s Manual, (November).

Seibert, J., & Vis, M. J. P. (2012). Teaching hydrological modeling with a user-friendly catchment-runoff-model software package. *Hydrology and Earth System Sciences*, *16*(9), 3315–3325. doi:10.5194/hess-16-3315-2012

Setegn, S. G., Rayner, D., Melesse, A. M., Dargahi, B., Srinivasan, R., & Wörman, A. (2011). Nile River Basin, 241–265. doi:10.1007/978-94-007-0689-7

SMHI. (2008). Manual, *6.0*.

Solomatine, D. P., & Shrestha, D. L. (2009). A novel method to estimate model uncertainty using machine learning techniques. *Water Resources Research*, *45*, 1–16. doi:10.1029/2008WR006839

Stisen, S., & Sandholt, I. (2010). Evaluation of remote-sensing-based rainfall products through predictive capability in hydrological runoff modelling. *Hydrological Processes*, *24*(7), 879–891. doi:10.1002/hyp.7529

Su, F., Hong, Y., & Lettenmaier, D. P. (2008). Evaluation of TRMM Multisatellite Precipitation Analysis (TMPA) and Its Utility in Hydrologic Prediction in the La Plata Basin. *Journal of Hydrometeorology*, *9*, 622–640. doi:10.1175/2007JHM944.1

Tobin, K. J., & Bennett, M. E. (2010). Adjusting Satellite Precipitation Data to Facilitate Hydrologic Modeling. *Journal of Hydrometeorology*, *11*, 966–978. doi:10.1175/2010JHM1206.1

Worqlul, a. W., Maathuis, B., Adem, a. a., Demissie, S. S., Langan, S., & Steenhuis, T. S. (2014). Comparison of TRMM, MPEG and CFSR rainfall estimation with the ground observed data for the Lake Tana Basin, Ethiopia. *Hydrology and Earth System Sciences Discussions*, *11*, 8013–8038. doi:10.5194/hessd-11-8013-2014

APPENDICES

APPENDIX A: Rainfall station consistency check – Double Mass Curves

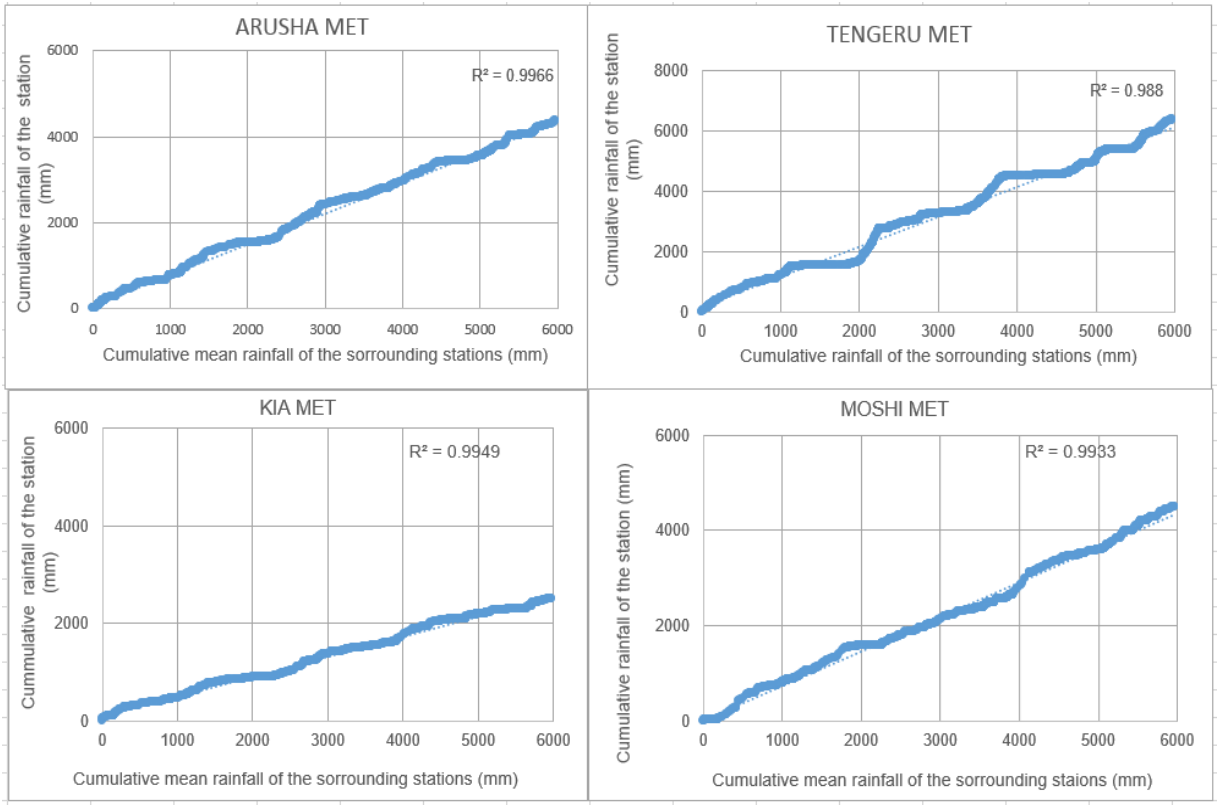

APPENDIX B:

Hyrdo-meteorological stations within the catchment. **Top**: manual and automatic water level stations at (IDDI), **Bottom**: Nafco-Kahe meteorological station.

APPENDIX C:

Separation of the base-flow from the total runoff to obtain quick runoff.

Date	Base-flow ($m^3 s^{-1}$)	Runoff ($m^3 s^{-1}$)	Date	Base-flow ($m^3 s^{-1}$)	Runoff ($m^3 s^{-1}$)	Date	Base-flow ($m^3 s^{-1}$)	Runoff ($m^3 s^{-1}$)
01/01/2010	16.71	0	16/02/2010	12.86	0	03/04/2010	29.06	68.16
02/01/2010	15.50	0	17/02/2010	12.86	0	04/04/2010	30.00	21.91
03/01/2010	14.36	0	18/02/2010	12.49	0	05/04/2010	30.27	2.77
04/01/2010	13.79	0	19/02/2010	12.86	1.12	06/04/2010	30.32	0.46
05/01/2010	15.49	3.35	20/02/2010	12.88	1.09	07/04/2010	28.11	0
06/01/2010	15.60	3.85	21/02/2010	12.99	8.92	08/04/2010	33.36	0.38
07/01/2010	15.69	2.57	22/02/2010	13.10	2.01	09/04/2010	33.77	28.59
08/01/2010	15.77	2.49	23/02/2010	13.14	1.59	10/04/2010	34.28	10.36
09/01/2010	15.85	1.81	24/02/2010	13.16	0.07	11/04/2010	34.55	6.21
10/01/2010	15.94	4.93	25/02/2010	13.16	0.07	12/04/2010	34.98	26.82
11/01/2010	16.28	26.15	26/02/2010	13.16	0.07	13/04/2010	35.49	14.64
12/01/2010	16.72	15.65	27/02/2010	12.86	0	14/04/2010	35.94	21.74
13/01/2010	16.97	8.97	28/02/2010	13.12	0.11	15/04/2010	36.39	15.93
14/01/2010	17.11	4.18	01/03/2010	13.15	1.97	16/04/2010	36.84	22.36
15/01/2010	17.16	0.70	02/03/2010	13.18	0.80	17/04/2010	37.40	27.61
16/01/2010	14.93	0.00	03/03/2010	13.20	1.15	18/04/2010	37.84	10.73
17/01/2010	15.17	3.27	04/03/2010	13.22	0.38	19/04/2010	38.04	5.36
18/01/2010	15.23	2.22	05/03/2010	13.23	0.00	20/04/2010	38.21	8.88
19/01/2010	15.26	1.40	06/03/2010	13.27	3.78	21/04/2010	38.33	0.04
20/01/2010	15.29	0.98	07/03/2010	13.31	0.29	22/04/2010	36.26	0
21/01/2010	15.31	0.58	08/03/2010	13.33	1.40	23/04/2010	36.33	4.29
22/01/2010	15.32	0.76	09/03/2010	13.35	0.62	24/04/2010	36.44	4.54
23/01/2010	15.31	0	10/03/2010	13.36	0.24	25/04/2010	36.52	0.68
24/01/2010	14.74	0	11/03/2010	13.23	0	26/04/2010	34.41	0
25/01/2010	14.36	0	12/03/2010	13.24	0.74	27/04/2010	37.22	0
26/01/2010	14.36	0	13/03/2010	13.23	0	28/04/2010	38.15	0
27/01/2010	14.36	0	14/03/2010	13.23	0	29/04/2010	46.96	67.48
28/01/2010	14.36	0	15/03/2010	13.23	0	30/04/2010	48.85	97.66
29/01/2010	14.36	0	16/03/2010	12.86	0	01/05/2010	50.98	94.27
30/01/2010	13.98	0	17/03/2010	24.98	37.65	02/05/2010	52.38	29.54
31/01/2010	13.98	0	18/03/2010	25.81	22.76	03/05/2010	53.12	31.07
01/02/2010	13.60	0	19/03/2010	26.42	16.98	04/05/2010	54.12	56.62
02/02/2010	13.60	0	20/03/2010	26.99	20.10	05/05/2010	55.06	27.41
03/02/2010	13.63	0.73	21/03/2010	27.50	10.87	06/05/2010	55.69	27.34
04/02/2010	13.23	0	22/03/2010	27.88	8.38	07/05/2010	56.16	13.13
05/02/2010	13.23	0	23/03/2010	28.28	12.34	08/05/2010	56.40	5.96
06/02/2010	12.86	0	24/03/2010	28.70	12.28	09/05/2010	56.64	13.19
07/02/2010	12.97	0.26	25/03/2010	29.08	8.12	10/05/2010	56.86	5.50
08/02/2010	12.99	1.36	26/03/2010	29.38	5.03	11/05/2010	56.95	0.72
09/02/2010	13.02	1.71	27/03/2010	29.67	7.55	12/05/2010	56.13	0
10/02/2010	13.05	0.93	28/03/2010	29.99	8.17	13/05/2010	51.30	0
11/02/2010	13.07	0.54	29/03/2010	31.06	83.38	14/05/2010	51.51	19.32
12/02/2010	13.07	0.16	30/03/2010	33.16	113.35	15/05/2010	51.83	11.34
13/02/2010	12.86	0	31/03/2010	34.91	51.79	16/05/2010	51.96	1.37
14/02/2010	12.95	1.79	01/04/2010	27.02	0	17/05/2010	51.55	0
15/02/2010	12.98	1.38	02/04/2010	28.15	17.08	18/05/2010	47.80	0

Date	Base-flow ($m^3 s^{-1}$)	Runoff ($m^3 s^{-1}$)	Date	Base-flow ($m^3 s^{-1}$)	Runoff ($m^3 s^{-1}$)	Date	Base-flow ($m^3 s^{-1}$)	Runoff ($m^3 s^{-1}$)
19/05/2010	45.83	0	05/07/2010	21.91	0	21/08/2010	15.12	0.38
20/05/2010	42.91	0	06/07/2010	21.93	0.60	22/08/2010	15.13	0.56
21/05/2010	40.74	0	07/07/2010	21.94	0.38	23/08/2010	15.14	0.17
22/05/2010	41.47	0	08/07/2010	21.08	0	24/08/2010	15.12	0
23/05/2010	42.23	13.12	09/07/2010	20.87	0	25/08/2010	14.73	0
24/05/2010	42.57	18.22	10/07/2010	20.87	0	26/08/2010	14.54	0
25/05/2010	42.86	8.69	11/07/2010	20.46	0	27/08/2010	14.56	0.17
26/05/2010	43.00	4.07	12/07/2010	20.26	0	28/08/2010	14.57	0.17
27/05/2010	42.91	0	13/07/2010	20.06	0	29/08/2010	14.57	0.16
28/05/2010	42.98	6.08	14/07/2010	19.85	0	30/08/2010	14.58	0.35
29/05/2010	43.11	6.43	15/07/2010	19.04	0	31/08/2010	14.54	0
30/05/2010	43.20	2.39	16/07/2010	18.44	0	01/09/2010	14.55	0.18
31/05/2010	43.23	0.17	17/07/2010	18.24	0	02/09/2010	14.55	0
01/06/2010	40.51	0	18/07/2010	18.25	0.19	03/09/2010	13.79	0
02/06/2010	39.32	0	19/07/2010	18.26	0.19	04/09/2010	13.81	0.36
03/06/2010	38.61	0	20/07/2010	18.24	0	05/09/2010	13.81	0.17
04/06/2010	37.67	0	21/07/2010	17.25	0	06/09/2010	13.42	0
05/06/2010	37.68	0.22	22/07/2010	16.66	0	07/09/2010	13.42	0
06/06/2010	37.69	0.45	23/07/2010	16.66	0	08/09/2010	13.48	0.13
07/06/2010	36.96	0	24/07/2010	16.68	0.18	09/09/2010	13.48	0.31
08/06/2010	35.80	0	25/07/2010	16.68	0.37	10/09/2010	13.50	0.86
09/06/2010	35.10	0	26/07/2010	16.66	0	11/09/2010	13.52	1.03
10/06/2010	33.72	0	27/07/2010	16.66	0	12/09/2010	13.53	0.45
11/06/2010	33.50	0	28/07/2010	16.27	0	13/09/2010	13.42	0
12/06/2010	33.04	0	29/07/2010	16.27	0	14/09/2010	13.45	0.72
13/06/2010	32.13	0	30/07/2010	16.08	0	15/09/2010	13.46	0.34
14/06/2010	30.78	0	31/07/2010	15.88	0	16/09/2010	13.42	0
15/06/2010	28.99	0	01/08/2010	15.90	0.38	17/09/2010	13.05	0
16/06/2010	29.00	0	02/08/2010	15.69	0	18/09/2010	13.08	0.34
17/06/2010	29.00	0.22	03/08/2010	15.12	0	19/09/2010	13.09	0.70
18/06/2010	28.33	0	04/08/2010	15.18	0.32	20/09/2010	13.11	0.50
19/06/2010	28.33	0.00	05/08/2010	15.19	0.31	21/09/2010	12.86	0
20/06/2010	28.33	0	06/08/2010	15.20	0.50	22/09/2010	13.01	0.04
21/06/2010	28.33	0	07/08/2010	15.21	0.68	23/09/2010	13.02	0.22
22/06/2010	27.24	0	08/08/2010	15.22	0.66	24/09/2010	13.03	0.58
23/06/2010	26.58	0	09/08/2010	15.23	0.27	25/09/2010	13.04	0.57
24/06/2010	26.59	0.21	10/08/2010	14.93	0	26/09/2010	13.05	0.55
25/06/2010	25.50	0	11/08/2010	15.04	0.65	27/09/2010	13.06	0.17
26/06/2010	25.51	0.21	12/08/2010	15.05	0.26	28/09/2010	13.08	1.09
27/06/2010	25.52	0.20	13/08/2010	15.06	0.44	29/09/2010	13.10	0.88
28/06/2010	25.50	0	14/08/2010	15.07	0.05	30/09/2010	13.12	0.49
29/06/2010	24.65	0	15/08/2010	15.08	0.81	01/10/2010	13.13	0.48
30/06/2010	24.43	0	16/08/2010	15.09	0.60	02/10/2010	13.13	0.28
01/07/2010	23.16	0	17/08/2010	15.10	0.20	03/10/2010	13.14	0.28
02/07/2010	23.16	0	18/08/2010	15.11	0.01	04/10/2010	13.14	0.09
03/07/2010	22.33	0	19/08/2010	15.11	0.39	05/10/2010	13.15	0.09
04/07/2010	22.33	0.20	20/08/2010	15.12	0.19	06/10/2010	13.15	0.45

Date	Base-flow ($m^3 s^{-1}$)	Runoff ($m^3 s^{-1}$)	Date	Base-flow ($m^3 s^{-1}$)	Runoff ($m^3 s^{-1}$)
07/10/2010	13.05	0	19/11/2010	13.07	1.85
08/10/2010	12.86	0	20/11/2010	13.12	2.38
09/10/2010	12.98	0.62	21/11/2010	13.16	1.58
10/10/2010	13.00	0.42	22/11/2010	13.19	1.17
11/10/2010	13.00	0.23	23/11/2010	13.21	0.59
12/10/2010	13.01	0.22	24/11/2010	13.21	0.02
13/10/2010	13.03	1.14	25/11/2010	13.05	0
14/10/2010	13.05	0.93	26/11/2010	12.49	0
15/10/2010	13.05	0	27/11/2010	12.49	0
16/10/2010	13.06	0.92	28/11/2010	12.49	0
17/10/2010	13.07	0.72	29/11/2010	12.49	0
18/10/2010	12.86	0	30/11/2010	12.53	0.34
19/10/2010	12.68	0	01/12/2010	12.54	0.70
20/10/2010	12.72	0.32	02/12/2010	12.55	0.31
21/10/2010	12.73	0.31	03/12/2010	12.49	0
22/10/2010	12.74	0.31	04/12/2010	12.49	0
23/10/2010	12.75	0.30	05/12/2010	12.55	1.43
24/10/2010	12.75	0.48	06/12/2010	12.56	0.30
25/10/2010	12.76	0.29	07/12/2010	12.49	0
26/10/2010	12.68	0	08/12/2010	13.44	0.73
27/10/2010	12.68	0.18	09/12/2010	13.59	12.56
28/10/2010	12.68	0	10/12/2010	13.78	4.86
29/10/2010	12.73	0.32	11/12/2010	13.90	5.75
30/10/2010	12.73	0.13	12/12/2010	14.03	6.63
31/10/2010	12.74	0.31	13/12/2010	14.16	5.29
01/11/2010	12.75	0.67	14/12/2010	14.26	3.99
02/11/2010	12.76	0.29	15/12/2010	14.31	1.39
03/11/2010	12.77	0.46	16/12/2010	14.17	0
04/11/2010	12.68	0	17/12/2010	13.98	0
05/11/2010	12.68	0	18/12/2010	13.42	0
06/11/2010	12.72	0.14	19/12/2010	13.43	0.17
07/11/2010	12.72	0.51	20/12/2010	13.44	0.54
08/11/2010	12.74	0.50	21/12/2010	13.42	0
09/11/2010	12.74	0.30	22/12/2010	12.68	0
10/11/2010	12.75	0.30	23/12/2010	12.49	0
11/11/2010	12.68	0	24/12/2010	12.49	0
12/11/2010	12.49	0	25/12/2010	12.56	0.67
13/11/2010	12.67	0.00	26/12/2010	12.58	1.40
14/11/2010	12.68	0	27/12/2010	12.61	0.81
15/11/2010	12.87	0.73	28/12/2010	12.49	0
16/11/2010	12.90	1.46	29/12/2010	12.54	1.44
17/11/2010	12.95	2.94	30/12/2010	12.49	0
18/11/2010	13.02	3.07	31/12/2010	12.49	0